Investigating fossil hydrothermal systems by means of fluid inclusions and stable isotopes in banded travertine: an example from

Investigating fossil hydrothermal systems by means of fluid inclusions and stable isotopes in banded travertine: an example from Castelnuovo dell'Abate (southern Tuscany, Italy)

Valentina Rimondi, Pilario Costagliola, Giovanni Ruggieri, Marco Benvenuti, Chiara Boschi, Andrea Brogi, Enrico Capezzuoli, et al.

International Journal of Earth Sciences
GR Geologische Rundschau

ISSN 1437-3254

Int J Earth Sci (Geol Rundsch)
DOI 10.1007/s00531-015-1186-y

Springer

Int J Earth Sci (Geol Rundsch)
DOI 10.1007/s00531-015-1186-y

ORIGINAL PAPER

Investigating fossil hydrothermal systems by means of fluid inclusions and stable isotopes in banded travertine: an example from Castelnuovo dell'Abate (southern Tuscany, Italy)

Valentina Rimondi[1] · Pilario Costagliola[2] · Giovanni Ruggieri[1] · Marco Benvenuti[2] · Chiara Boschi[3] · Andrea Brogi[4] · Enrico Capezzuoli[5] · Guia Morelli[6] · Massimo Gasparon[6,7] · Domenico Liotta[4]

Received: 29 September 2014 / Accepted: 26 April 2015

Abstract Southern Tuscany (Italy) hosts geothermal anomalies with associated widespread CO_2 gas-rich manifestations and active travertine-deposing thermal springs. Geothermal anomalies have been active since the Late Miocene and have led to the formation of widespread Late Miocene–Pleistocene travertine deposits and meso- and epithermal mineralizations. This study investigates the travertine deposit exposed in the Castelnuovo dell'Abate area of southern Tuscany. Here, a fissure-ridge type travertine deposit and its feeding conduits, currently filled with banded calcite veins (i.e. banded travertine), represent a spectacular example of fossil hydrothermal circulation in the peripheral area of the exploited Monte Amiata geothermal field. The Castelnuovo dell'Abate travertine deposit and associated calcite veins were analysed to establish the characteristics of the parent hydrothermal fluids, and the age of this circulation. The focus of the study was on fluid inclusions, rarely considered in travertine studies, but able to provide direct information on the physico-chemical characteristics of the original fluid. Uranium–thorium geochronological data provided further constraints on the: (1) age of tectonic activity; (2) age of the hydrothermal circulation; and (3) evolution of the Monte Amiata geothermal anomaly. Results indicate that brittle deformation (NW- and SE-trending normal to oblique-slip faults) was active during at least the Middle Pleistocene and controlled a hydrothermal circulation mainly characterized by fluids of meteoric origin, and as old as 300–350 ka. This is the oldest circulation documented to date in the Monte Amiata area. The fluid chemical composition is comparable to that of fluids currently exploited in the shallow reservoir of the Monte Amiata geothermal field, therefore suggesting that fluid composition has not changed substantially over time. These fluids, however, have cooled by about 70 °C in the last 300–350 ka, corresponding to a cooling rate of the Monte Amiata geothermal area of about 20 °C 100 ka^{-1}.

Keywords Banded travertine · C and O isotope geochemistry · Fluid inclusions study · Monte Amiata geothermal field

✉ Valentina Rimondi
valentina.rimondi@unifi.it

1 CNR - Istituto di Geoscienze e Georisorse, Via G. La Pira 4, 50121 Florence, Italy

2 Dipartimento di Scienze della Terra, Università di Firenze, Via G. La Pira 4, 50121 Florence, Italy

3 CNR - Istituto di Geoscienze e Georisorse, Via Moruzzi 1, 56124 Pisa, Italy

4 Dipartimento di Scienze della Terra e Geoambientali, Università di Bari, Via Orabona 4, 70125 Bari, Italy

5 Dipartimento di Fisica e Geologia, Università di Perugia, Via Pascoli, 06123 Perugia, Italy

6 School of Earth Sciences, The University of Queensland, St Lucia, QLD 4072, Australia

7 Australian National Centre for Groundwater Research and Training, The University of Queensland, St Lucia, QLD 4072, Australia

Introduction

The term "terrestrial carbonates" encompasses a wide spectrum of lithotypes mainly originated from calcium bicarbonate-rich waters under subaerial conditions, in a large variety of depositional and diagenetic settings (Flügel 2004). According to several classifications, the term "travertine" indicates continental limestone deposited from non-marine, supersaturated calcium bicarbonate-rich waters,

Published online: 20 May 2015

discharging to the surface from a deep geothermal system (Riding 1991; Ford and Pedley 1996; Fouke et al. 2000; Capezzuoli et al. 2014; Gandin and Capezzuoli 2014).

Southern Tuscany is characterized by a broad geothermal anomaly (Della Vedova et al. 2001) that is mainly centred in the Larderello-Travale and Monte Amiata geothermal areas (Batini et al. 2003) and strictly associated with CO_2 leakage and travertine deposits (Rogie et al. 2000; Minissale 2004). The geothermal systems of southern Tuscany mainly consist of two main reservoirs occurring at shallow crustal levels. The deeper reservoir (*T* of 300–350 °C, depth 1000–3000 m) is hosted in metamorphic rocks, while the shallower reservoir (*T* lower than 200 °C, depth 500–1000 m) is hosted mainly in carbonate rocks (Duchi et al. 1992; Batini et al. 2003). Travertine deposits are the surface manifestation of hydrothermal fluid circulation within the carbonate reservoirs (Brogi et al. 2015 and reference therein) and are widely distributed in southern Tuscany and northern Latium (Minissale 2004, Brogi et al. 2010a, 2012; Capezzuoli et al. 2011). Over the last decade, ongoing research mainly focused on the inactive (i.e. fossil) depositional systems for neotectonic and palaeoseismological issues (Altunel and Karabacak 2005; Brogi and Capezzuoli 2009; Brogi et al. 2010a, 2012, 2014; De Filippis et al. 2013; Uysal et al. 2007), as well as for palaeoclimate reconstructions (Manfra et al. 1974; Faccenna et al. 2008).

The study of fluid inclusions represents a unique technique for the reconstruction of the physical and chemical characteristics of the travertine parent fluid and its depositional environment. However, the application of this technique to travertine deposits is rather new (Słowakiewicz 2003; Gibert et al. 2009; El Desouky et al. 2015) and has not been attempted before on Italian deposits. Fluid inclusions investigation in travertine is potentially complicated by: (1) the generally small size of the fluid inclusions (Pentecost 2005); (2) their metastability, which prevents the nucleation of the bubble upon cooling from the trapping conditions to room temperature (Shepherd et al. 1985; Diamond 2003); (3) the intrinsic difficulties in performing microthermometric analysis in calcite, which is often subjected to anelastic stretching phenomena (Roedder 1984; Shepherd et al. 1985), that may lead to misinterpretation of the results. This study is the first successful application of the fluid inclusions methodology to calcites, formed in the inactive (i.e. fossil) Pleistocene hydrothermal system of Castelnuovo dell'Abate in southern Tuscany (Fig. 1a, b). Here, a spectacular network of banded calcite veins cross-cutting both a fissure-ridge type travertine deposit and its substratum is exposed in an abandoned quarry. The travertine was further characterized in terms of its mineralogy, geochemistry, C and O isotopic composition, and age using U-series dating. The results provide information on the age of the tectonic activity and hydrothermal circulation. Combined with previous studies on active and fossil neighbouring hydrothermal systems (Frondini et al. 2009; Gasparrini et al. 2013), these results provide new insights into the evolution of the shallow hydrothermal reservoir of the Monte Amiata region and its possible cooling rate during the last 300–400 ka.

Geological setting

The Monte Amiata Middle–Late Pleistocene volcanic complex (Ferrari et al. 1996; Cadoux and Pinti 2009) is located in the inner Northern Apennines (Fig. 1a), a Tertiary (Late Cretaceous–Early Miocene) belt derived from the convergence and collision between the Adria microplate and the European plate (Molli 2008 and references therein) and its interplay with the opening of the Tyrrhenian Basin (Bartole 1995). After the stacking of the tectonic units, extensional tectonics (Carmignani et al. 1994; Brogi et al. 2005) and coeval magmatism (Peccerillo 2003; Dini et al. 2005) affected the previously overthickened continental crust since the Early–Middle Miocene (Brunet et al. 2000) and led to the exhumation of deeper tectonic units (Carmignani et al. 1995), widespread geothermal anomalies (Della Vedova et al. 2001) and hydrothermal circulation (Tanelli 1983). Around Monte Amiata, hydrothermal circulation was responsible for the world-class Hg and Sb deposits, extensively mined up to thirty years ago (Rimondi et al. 2015), as well as to barren hydrothermal calcite veins (Gasparrini et al. 2013). Hydrothermal fluid flow is still active in this area as manifested by the travertine deposition from thermal springs at Bagno Vignoni and Bagni San Filippo (Fig. 1a), the occurrence of numerous CO_2-rich gas emissions (Frondini et al. 2009) and the two geothermal fields (Bagnore and Piancastagnaio) exploited for electricity production (Batini et al. 2003). All these features can be related to the thermal anomaly generated by a granitoid cooling at about 6–7 km below sea level (Gianelli et al. 1988; Bertini et al. 1995; Brogi 2008).

Hydrothermal circulation in the Monte Amiata area (i.e. Hg mineralization, thermal springs, travertine deposits and gas emissions) has mainly been controlled by normal faults and their associated transfer zones, trending NW and NE, respectively (Brogi et al. 2010b). Similarly, at Castelnuovo dell'Abate, the travertine deposit is aligned with a N50° trending fault (Fig. 1b), which is interpreted as a transfer zone and played the role of the main conduit that channelled the feeding hydrothermal fluids. This fault separates Late Oligocene–Early Miocene quartz-feldspar sandstone (Macigno Fm) belonging to the Tuscan Nappe, from the overlying Cretaceous marl and marly limestone (S. Fiora Fm) belonging to the Ligurian units (Fig. 2).

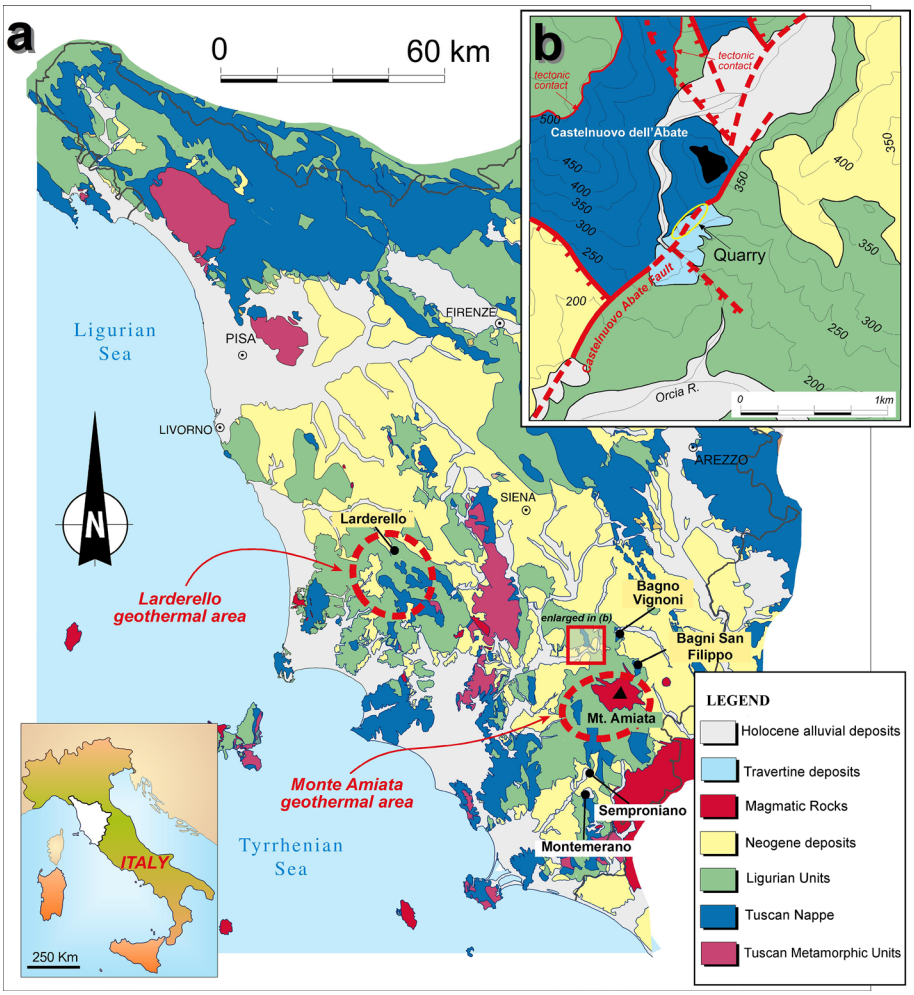

Fig. 1 **a** Geologic map of southern Tuscany and main geothermal features; the present-day travertine deposits associated with active thermal springs are also indicated (Bagno Vignoni and Bagni San Filippo); **b** geological map of Castelnuovo dell'Abate and surrounding area

Castelnuovo dell'Abate travertine and banded calcite vein system

The Castelnuovo dell'Abate travertine depositional system crops out about 300 m south of the homonymous village (Fig. 1b) and can be described as a fissure-ridge depositional system (Fig. 3). Travertine and related banded calcite were intensively exploited for ornamental use for centuries, and this made it possible to study their general features on the faces of the many abandoned quarries. The whole travertine body was affected by brittle deformation that caused intense fracturing and faulting.

According to Altunel and Hancock's (1993) classification, two main depositional associations have been recognized: bedded and banded travertine (Fig. 3), the latter consisting of: (1) banded calcite veins filling the vertical, straight-to-sinuous fissure crossing the central part of the (eroded) fissure-ridge body (Fig. 3), and (2) sub-horizontal to sub-vertical banded calcite veins intruded within the substratum (limestone and marl of the S. Fiora Fm and conglomerate), often showing mutual crosscutting relationships due to hydrofracturing (Fig. 4). Banded calcite veins represent most of the travertine body and consist of crystalline, laminated crusts (Fig. 5a) precipitated in hypogean conditions. These are formed by onyx-like, well-banded, centimetre-to-metre-thick, white-to-brown calcite bands (Fig. 5b). Bands are formed by palisade, fibrous or blocky prismatic crystals grown in syntaxial continuity (Fig. 5a). Sub-horizontal veins follow closely the geometry of the beds of the hosting limestone and marl forming the travertine substratum, like sills (Fig. 4d–f). Pinched (characterized by a V-shaped morphology; Fig. 5c) and highly brecciated bands are locally present and represent the evolution of superimposed fractures that changed their trajectories isolating lithons of previously deposited bedded travertine. Occasionally, centimetre-scale breccia fragments, cemented by interstitial calcite including light grey carbonatic fragments derived from the host, have been incorporated within the banded veins. The thickness of the banded calcite veins is extremely variable, ranging from some centimetres to a few decimetres in the travertine substratum. In contrast, their thickness varies from some millimetres to a

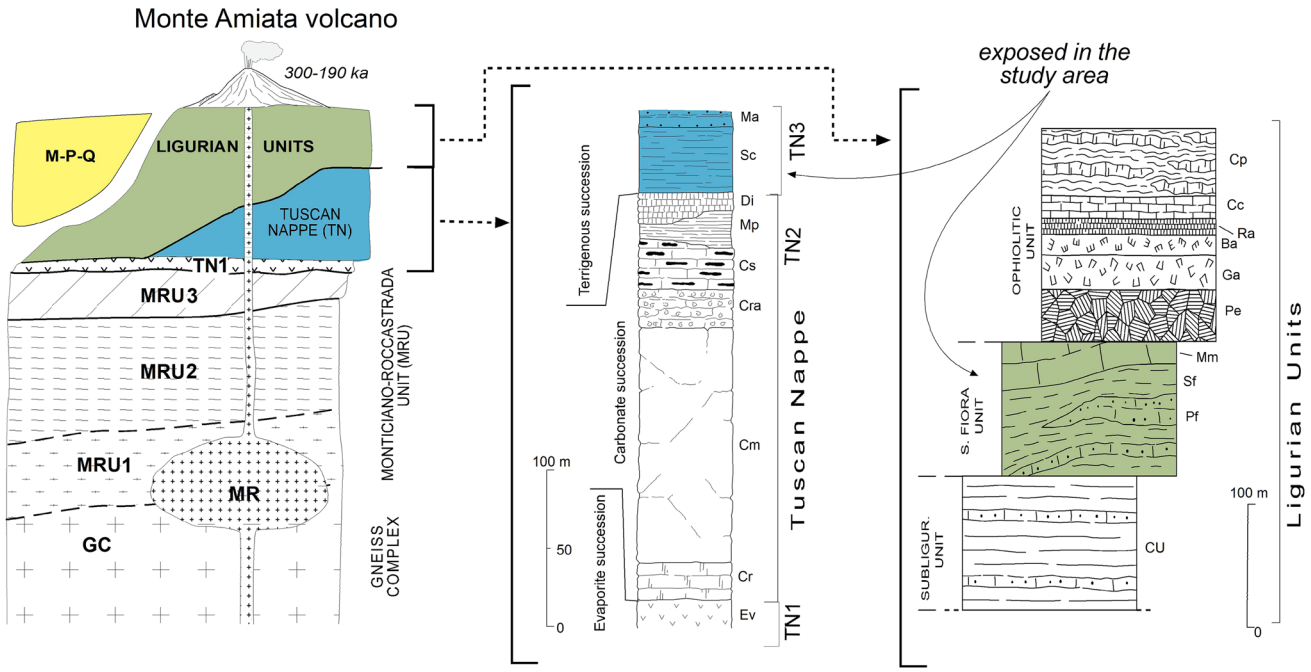

Fig. 2 Tectono-stratigraphic units in the study area (modified after Batini et al. 2003; Gasparrini et al. 2013); M–P–Q: Miocene, Pliocene and Quaternary sediments; MR—magmatic rocks; Tuscan Nappe (TN): TN3—Early Miocene–Cretaceous clayey-turbiditic succession; TN2—Cretaceous–Rhaetian carbonate succession, TN1—Late Triassic evaporite succession; Monticiano–Roccastrada Unit (MRU): MRU3—Triassic Verrucano Group; MRU2—Palaeozoic Phyllite–Quartzite Group; MRU1—Palaeozoic Micaschist Group; GC—Palaeozoic Gneiss Complex. Tuscan Nappe: Ev—Late Triassic evaporites (Burano Fm) composed of an alternation of dolostone and dolomitic limestone and gypsum layers often brecciated; Cr—Late Triassic carbonate succession (Calcari a Rhaetavicula contorta Fm) composed of Rhaetian dark limestone interbedded with decimetre thick marl and marly limestone; Cm—Early Jurassic massive grey limestone (Calcare Massiccio Fm); Cra—Early Jurassic red nodular limestone (Calcare Rosso Ammonitico Fm); Cs—Early Jurassic marly limestone and grey cherty limestone (Calcare Selcifero Fm); Mp—Middle Jurassic marl and marly limestone (Marne a Posidonia Fm); Di—Late Jurassic radiolarite (Diaspri Fm); Sc—Cretaceous–Oligocene shale, marl, limestone, calcarenite and calcirudite (Scaglia Toscana Fm); Ma—Late Oligocene–Early Miocene sandstone and shale (Macigno Fm). Ligurian Units: CU—Eocene–Oligocene limestone and shale (Canetolo Fm); Sf—Cretaceous limestone, marl and shale (S. Fiora Fm); Pf—Cretaceous sandstone (Pietraforte Fm); Mm—Palaeocene–Eocene marl and limestone (Monte Morello Fm); Pe—Jurassic peridotite; Ga—Jurassic gabbro; Ba—Jurassic basalt; Ra—Late Jurassic radiolarites (Diaspri Fm); Cc—Early Cretaceous siliceous limestone (Calcari a Calpionella Fm); Cp—Early Cretaceous shale and siliceous limestone (Calcari a Palombini)

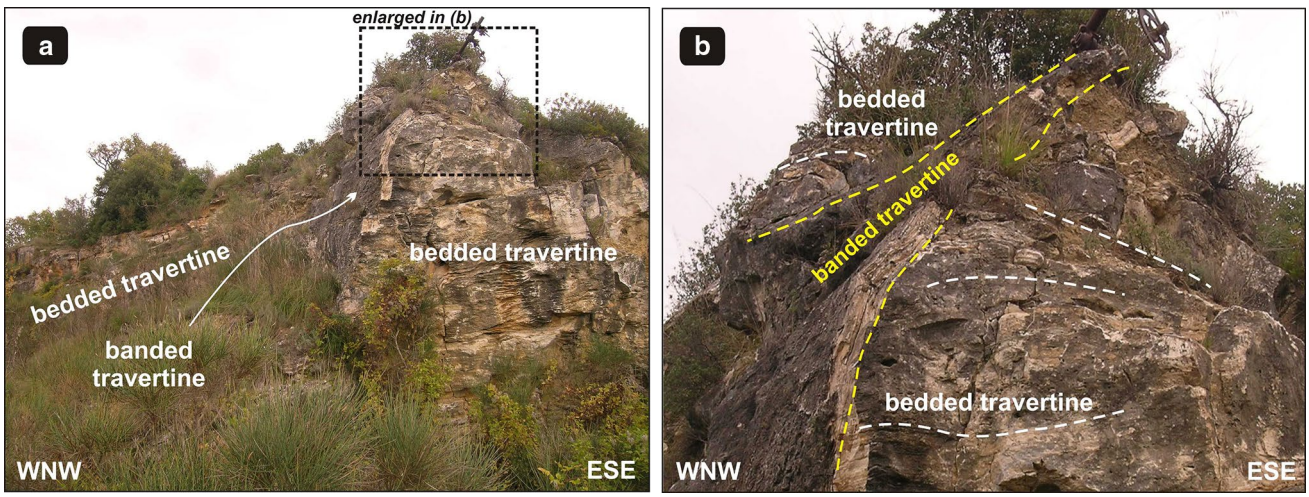

Fig. 3 **a** Panoramic view of some quarry faces showing part of the architectural components of the travertine fissure-ridge deposit; **b** detail of (**a**); banded travertine vein and opposite dipping walls made by bedded travertine can be recognized

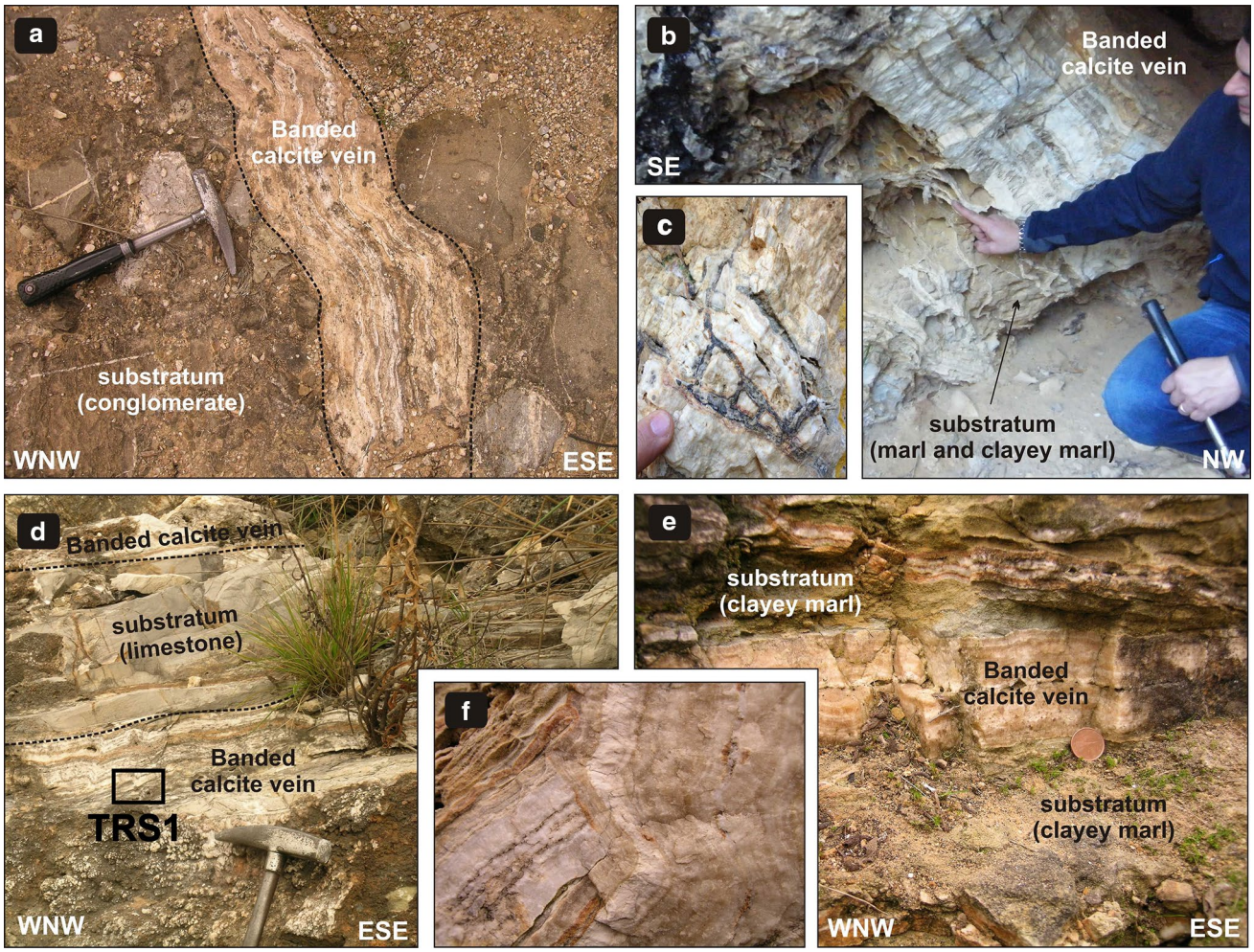

Fig. 4 **a** Banded calcite vein crosscutting the substratum of the fissure-ridge travertine deposit, made by conglomerate; **b** sub-vertical centimetre-to-decimetre-thick banded calcite veins crosscutting the substratum of the fissure-ridge travertine deposit, made by marl and clayey marl belonging to the Cretaceous S. Fiora Fm; **c** network of millimetre-thick banded calcite veins crosscutting a previous calcite vein, related to hydrofracturing; **d** sub-horizontal banded calcite veins (sill-like) parallel to limestone beds belonging to the Cretaceous S. Fiora Fm and location of sample TRS1; **e** sub-horizontal banded calcite veins (sill-like) with syntaxial geometry, parallel to marl beds belonging to the Cretaceous S. Fiora Fm; **f** crosscutting relationships between different generations of banded calcite veins

few metres (maximum values of about 3 m) in the central part of the fissure ridge, along the main trace of the fault.

The bedded travertine consists of scattered outcrops, in some cases representing metre-sized lithons embedded within banded calcite veins. It comprises variously inclined, wavy-crinkled laminated to non-stratified lithofacies deposited in epigean, proximal-to-distal conditions by the thermal waters flowing from the vent(s) along slopes (Fig. 5d). According to Gandin and Capezzuoli (2014), different types of crusts and granular facies with variable thickness and lateral evolution can be recognized (Fig. 5e, f). Such lateral facies organization, typical of a thermal depositional system (Guo and Riding 1998, 1999), provides evidence of different microenvironments (pools and shallow basins, microterraced slopes) repeatedly following one upon another.

Methods

Banded travertine was collected both in the substratum of the travertine body and in the travertine ridge (Figs. 4d, 5c) with the aim to characterize fluid circulation inside the travertine system. The same set of banded travertine samples (TRS1, TRS2/1 and TRS2/2) was analysed for fluid inclusions, mineralogy, C and O isotopes, and U-series dating. Materials for isotope analyses and dating were obtained from single bands by microdrilling. To this purpose, only bands that displayed a width larger than the drill tip were

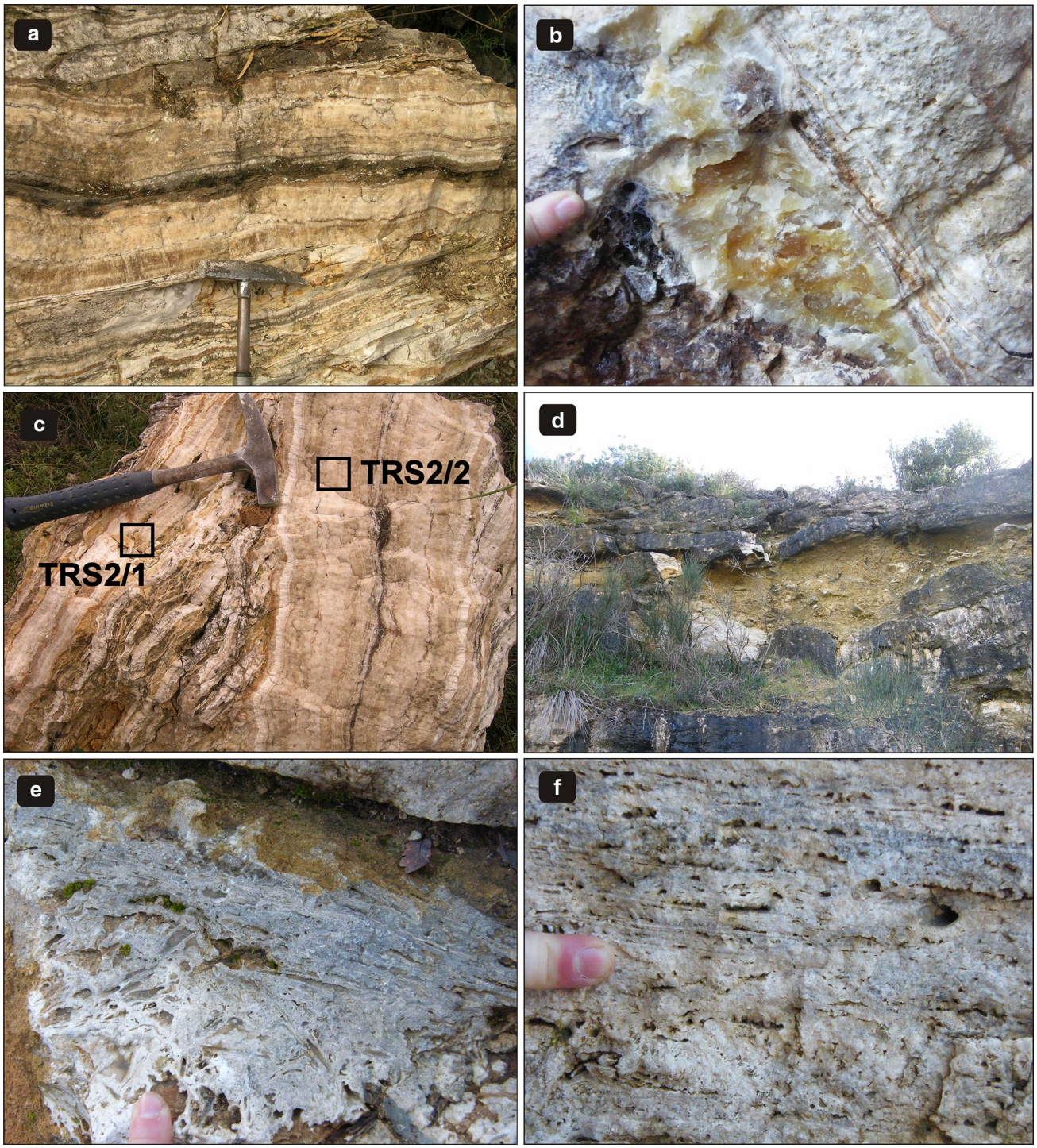

Fig. 5 **a** Typical aspect of banded travertine, formed by laminated, differently coloured calcite and with syntaxial geometry veins; **b** detailed view of a banded calcite veins, formed by mm-to-cm, prismatic-to palisade crystal calcite bands and characterized by different colors; **c** common feature of the banded travertine mutually crossing with V-shape aspect; location of samples TRS2/1 and TRS2/2 are reported; **d** alternation of crystalline crusts and detrital, sandy deposits documenting a slope environment; **e** encrusted reeds in horizontal position from a distal slope environment; **f** bedded travertine: superposition of paper-thin raft of pool environment

selected. Different bands were analysed for stable isotopes and U-series dating. Although these bands appear homogeneous at the scale of the hand specimen, it cannot be excluded that each sample represents a mixture of different depositional micro-events during travertine deposition. A more detailed investigation at the microscale was beyond

the scope of the present work, since the main goal was to obtain general information on the fluid characteristics and on the age of the hydrothermal system.

Fluid inclusions were studied in 70- to 100-μm-thick double-polished wafers of calcite samples. Particular care was taken during sample preparation to avoid or minimize anelastic calcite stretching; a low-speed trim saw was used for sample cutting, and little pressure was applied on the samples during grinding and polishing (Goldstein and Reynolds 1994).

Microthermometric measurements were performed using a Linkam THMSG600 heating–freezing stage coupled with a microscope Ortholux II POL-BK (Leitz) at the CNR-IGG in Firenze. The stage was calibrated by using pure H_2O with critical density and mixed H_2O–CO_2 (CO_2 25 % M) synthetic fluid inclusions. Accuracy was estimated to be ±0.2 °C for final ice melting temperature (Tm_{ice}) measurements and ±0.1 °C for homogenization temperature (Th). Due to the inelastic behaviour of calcite, heating generally preceded the freezing stage to avoid decrepitation and stretching phenomena commonly associated with volume expansion during ice formation (Roedder 1984). The temperature of homogenization was systematically measured only on liquid-rich inclusions. In vapour-rich inclusions, no remarkable increase in the liquid/vapour ratio was observed within the Th range of liquid-rich inclusions; thus, heating was stopped at 160 °C to overcome overheating phenomena and consequent decrepitation of liquid-rich inclusions.

The temperature of final ice melting was determined in liquid-rich inclusions, while Tm_{ice} was generally not observed in vapour-rich inclusions. The apparent salinity of fluid inclusions (Hedenquist and Henley 1985) was calculated from Tm_{ice} using the equation of Bodnar and Vytik (1994) and expressed in wt% NaCl eq. To assess the presence of non-condensable gases in the inclusions, a number of crushing tests was carried out (cf. Roedder 1970).

SEM–EDS analyses were carried out at the Centro Interdipartimentale di Microscopia Elettronica (MEMA, Firenze) on polished sections using a SEM/EDS ZEISS MA 15 and an acceleration potential of 25 kV.

Single bands were microdrilled along specific transects of calcite veins, orthogonal to vein direction, powdered if necessary and analysed for C and O isotopes. Calcite samples were analysed for $\delta^{13}C$ and $\delta^{18}O$ by using a Finnigan-MAT 252 (CNR-IGG in Pisa) after dissolution in phosphoric acid by using a common-acid bath technique at 70 °C (based on McCrea 1950). Data were corrected for the usual isobaric interferences following the procedure of Craig (1957) modified for a triple-collector instrument. The $\delta^{18}O$ value was calculated considering the acid fractionation factor and calibrated relative to the laboratory calcite standard (Friedman and O'Neil 1977). Carbon and oxygen isotope abundances are reported in δ values in per mill relative to the Vienna Peedee belemnite (V-PDB) and Standard Mean Oceanic Water (SMOW), respectively. The internal standards were measured at regular intervals within the sample set, and the uncertainty was less than 0.20 and 0.10 ‰ for $\delta^{13}C$ and $\delta^{18}O$, respectively.

For U-series dating, samples were washed with deionized water, cleaned in an ultrasonic bath to remove any possible contamination from the surface and dried at 40 °C on a hotplate. A total of five calcite bands were microdrilled using a bench drill, two bands from sample TRS1 (at 12 and 20 cm distance from the wall, labelled TRS1_12 and TRS1_20, respectively, the notation is applied to the other samples), one vein from sample TRS2/1 (at 25 cm from the wall) and one vein from sample TRS2/2 (at 35 and 90 cm from the wall). U–series dating was carried out in the Radiogenic Isotope Laboratory at the School of Earth Sciences (The University of Queensland) using a Nu Plasma multi-collector inductively coupled mass spectrometer (MC-ICP-MS). Samples (about 0.01 g powders) were completely dissolved using ultra-pure double-distilled concentrated HNO_3 mixed with a ^{229}Th–^{233}U spike. Hydrogen peroxide was added to the samples after digestion to remove any possible organic matter, and a new anion-exchange column chemistry procedure (modified after Edwards et al. 1987; Zhao et al. 2001; Clark et al. 2012) was used to purify U and Th. Unlike the procedure commonly used in the past, in this modified procedure, U and Th are eluted together using ~3 ml of a 1 % HNO_3 + 0.03 % HF mixture. The mixed solution was then directly injected through a DSN-100 desolvation system for simultaneous U and Th isotope measurement following the procedures first described in Zhou et al. (2011). Correction of initial ^{230}Th was done using a two-component correction scheme. The non-radiogenic ^{230}Th was corrected assuming a bulk-Earth atomic $^{230}Th/^{232}Th$ ratio of $4.4 \pm 2.2 \times 10^{-6}$, while $^{230}Th/^{238}U$ and $^{234}U/^{238}U$ activity ratios of the samples were calculated using the decay constants given in Cheng et al. (2000). Final U–Th ages were calculated using the Isoplot/Ex 3.0 Program (Ludwig 1999).

Results

Mineralogy

X-ray diffraction analysis (XRD) shows that the banded travertines are mainly composed of calcite (~90 wt%), and to a minor extent by phyllosilicates and quartz (~10 wt%). No aragonite was detected, suggesting that this mineral represents less than 5 %, if present. In transmitted light microscopy, calcite is commonly present as elongated

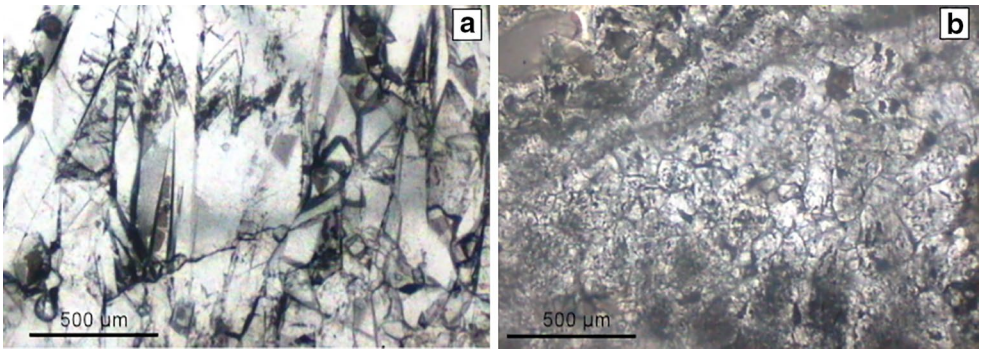

Fig. 6 Photomicrographs (transmitted light, parallel nicols) of elongated (**a**) and blocky (**b**) calcite in the Castelnuovo dell'Abate travertine

crystals fractured perpendicular to their accretional direction (Fig. 6a), or more rarely as small (around 50–100 µm) crystals with a blocky texture (Fig. 6b). Abundant opaque minerals mark the accretional margins of calcite, resulting in a typical "V" morphology in thin section (Fig. 7a). These phases were identified by SEM–EDS analysis as pyrite, Fe-(hydr)oxides, and/or pseudomorph Fe-(hydr)oxides after pyrite (Fig. 7b; Table 1). Two calcite vein samples (TRS2/1 and TRS2/2) contain fluorite (Fig. 7c) in discrete accretional bands along calcite blocky crystals. Celestine ($SrSO_4$) is an additional accessory mineral (Fig. 7d) that occupies intercrystalline spaces between calcite crystals. Calcite is generally pure, but with some elongated bands rich in Sr (Sr ~ 3 wt%, based on SEM–EDS semi-quantitative analysis) (Fig. 7d), and associated with celestine. Arsenic content is as high as 2–3 wt% in Fe-(hydr)oxides and pyrite (Fig. 7e; Table 1).

Fluid inclusions

Fluid inclusion types and petrography

In general, fluid inclusions are scarce in the examined calcite, although they were found in both elongated and blocky calcite crystals (Fig. 8a–d). At room temperature, fluid inclusions are two-phase (aqueous liquid plus vapour) liquid-rich (L1), vapour-rich (V) or more rarely only liquid (L2) (Fig. 9a–f). The absence of a vapour phase in the L2 inclusions probably results from failure of bubble nucleation due to metastability processes. Vapour-rich inclusions have variable vapour-to-liquid ratio and may occur as two-phase inclusions (vapour plus minor liquid; V1) or as apparently one-phase inclusions (vapour; V2), though a small amount of liquid, not visible under the microscope, may also be present. Groups of L1/L2 inclusions often show a three-dimensional random distribution, suggesting that they are primary in origin (Roedder 1984) and that can be considered fluid inclusion assemblages (FIA) according to Goldstein and Reynolds (1994). Single large size (relative to host crystal) L1 inclusions can be also considered primary in origin (Roedder 1984).

In elongated crystals, some inclusions are located in the accretion margins of calcite, describing the typical V-shape already mentioned for pyrite and Fe-(hydr)oxides (Figs. 7a, e, 9e), and indicating a primary origin according to the criteria of Roedder (1984). The size of the fluid inclusions ranges from 10 µm to 200 µm in the direction of the maximum length (Figs. 7a, 8c, d).

In the accretion margin of calcite, L1 inclusions are often scarce (maximum two inclusions per single crystal), whereas large dark inclusions are more frequent (Fig. 9d). Most of the latter should be considered as opened inclusions that lost their fluid upon wafer preparation. Some single inclusions, however, also have a small portion of liquid (Fig. 9e), indicating that they are actually V1 inclusions. Rare groups of inclusions, consisting of a few L1 inclusions sometimes associated with L2, and single isolated L1 inclusions occur in the internal part of the elongated calcite crystals, as well within blocky calcite crystals (Fig. 9c–f).

L1 and L2 inclusions usually show irregular shape, although in some cases they are more rounded, or mimic the rhombohedric shape of the host crystal (Fig. 9c). The size of fluid inclusions ranges from 3 µm up to 200 µm in the direction of the maximum length. In some cases, necking-down was suspected to have affected L1 inclusions. This process can explain the presence of the rare L2 inclusions coexisting with L1 inclusions.

Groups of L1/L2 inclusions are sometimes associated with large V1 and/or V2 inclusions in the internal part of the elongated calcite crystals (Fig. 9a). The genetic coexistence of L1, L2, V1 and V2 in elongated calcite is likely related to fluid immiscibility processes resulting from boiling or effervescence. The variable vapour-to-liquid ratio showed by V1 inclusions is a typical consequence of the contemporaneous trapping of liquid and vapour within single inclusion (i.e. heterogeneous trapping) under immiscibility conditions (Roedder 1984). The large single V1 and V2 inclusions in the accretion margins of calcite also

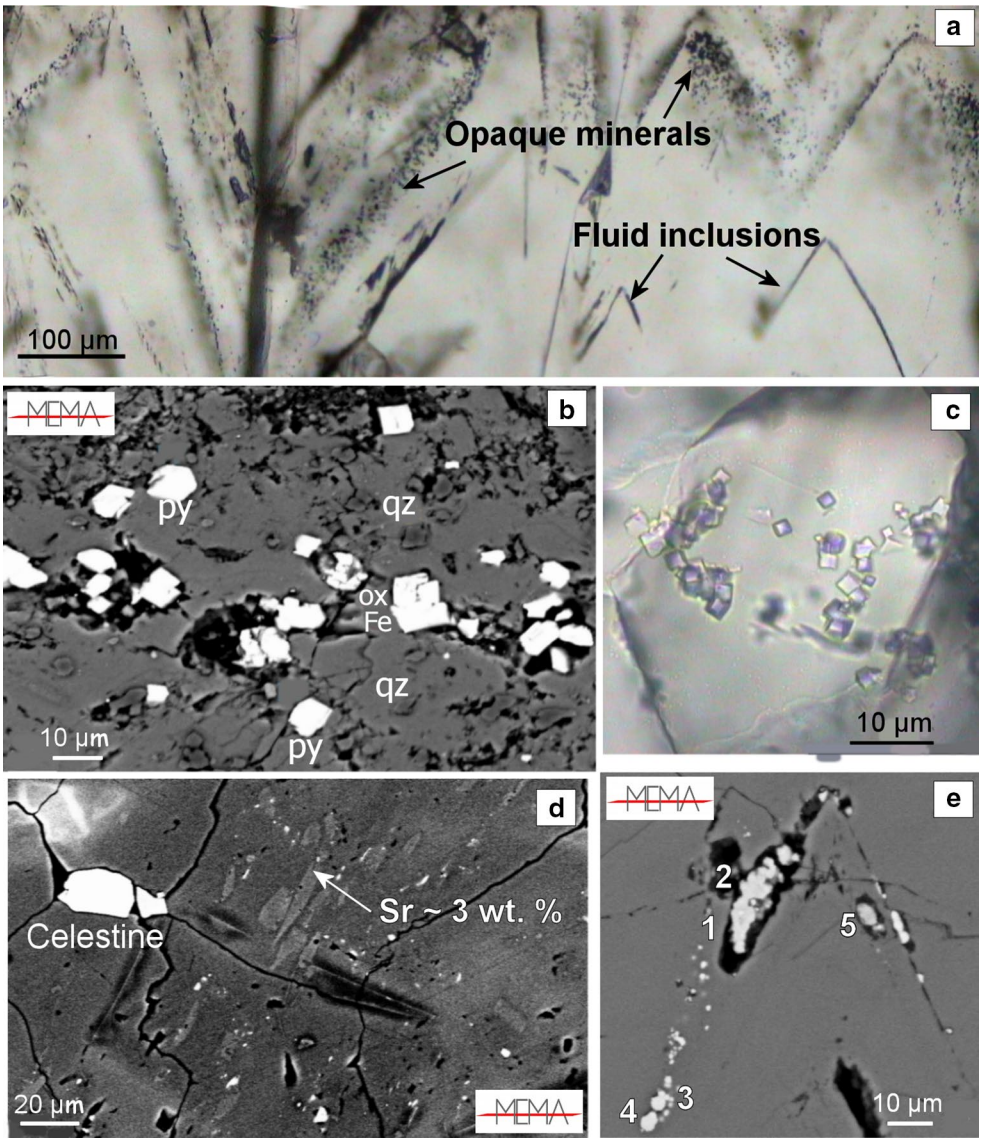

Fig. 7 Mineralogy of the Castelnuovo dell'Abate travertines (sample TRS2/2); **a** location of opaque minerals and fluid inclusions in the travertine thin sections (transmitted light microscopy, parallel nicols); **b** pyrite (py), Fe-oxides (ox Fe), and quartz (qz) (SEM, backscattered electron); **c** fluorite (transmitted light microscopy, parallel nicols); **d** celestine and Sr-enriched elongated bands in travertine calcite (SEM, backscattered electron); **e** detail of V-shaped opaque mineral assemblages of pyrite and Fe-oxides (SEM, backscattered electron). Point EDS analysis of the numbered phases are reported in Table 1

Table 1 SEM-EDS point analysis of As-rich mineral phases (Fe-(hydr)oxides and pyrites) numbered in Fig. 7e

Point analysis (Fig. 2e)	Mineral phase	Elements in wt%							
		O	Si	Al	S	Ca	Fe	As	Total
1	Fe-(hydr)oxides	30.2	2.6	3.9	–	4.6	56.8	1.9	100.0
2	Fe-(hydr)oxides	29.6	1.1	–	3.4	2.1	60.9	3.0	100.0
3	Pyrite	6.7	–	–	46.6	6.2	38.4	2.2	100.0
4	Pyrite	–	–	54.1	1.7	–	42.4	1.8	100.0
5	Fe-(hydr)oxides	30.2	2.6	3.9	–	4.6	56.8	1.9	100.0

Si, Al, O and Ca in the mineral detection are attributed to the neighbouring areas

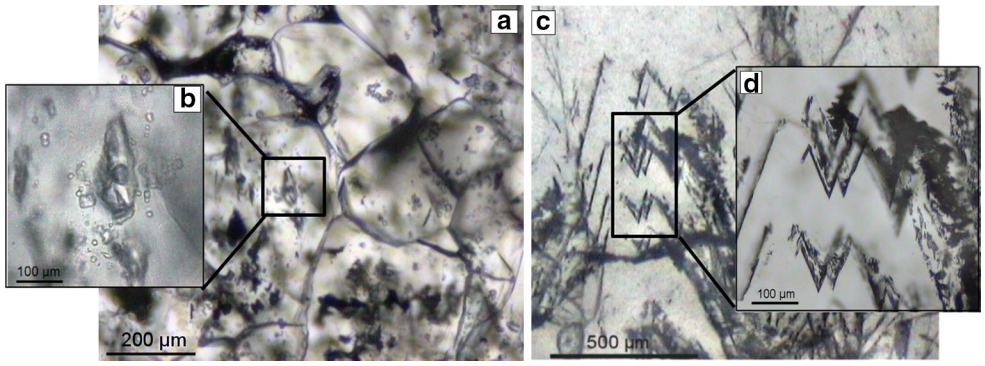

Fig. 8 Photomicrographs (transmitted light, parallel nicols) of fluid inclusions hosted in **a**, **b** blocky calcite, and **c**, **d** elongated calcite of the Castelnuovo dell'Abate travertine

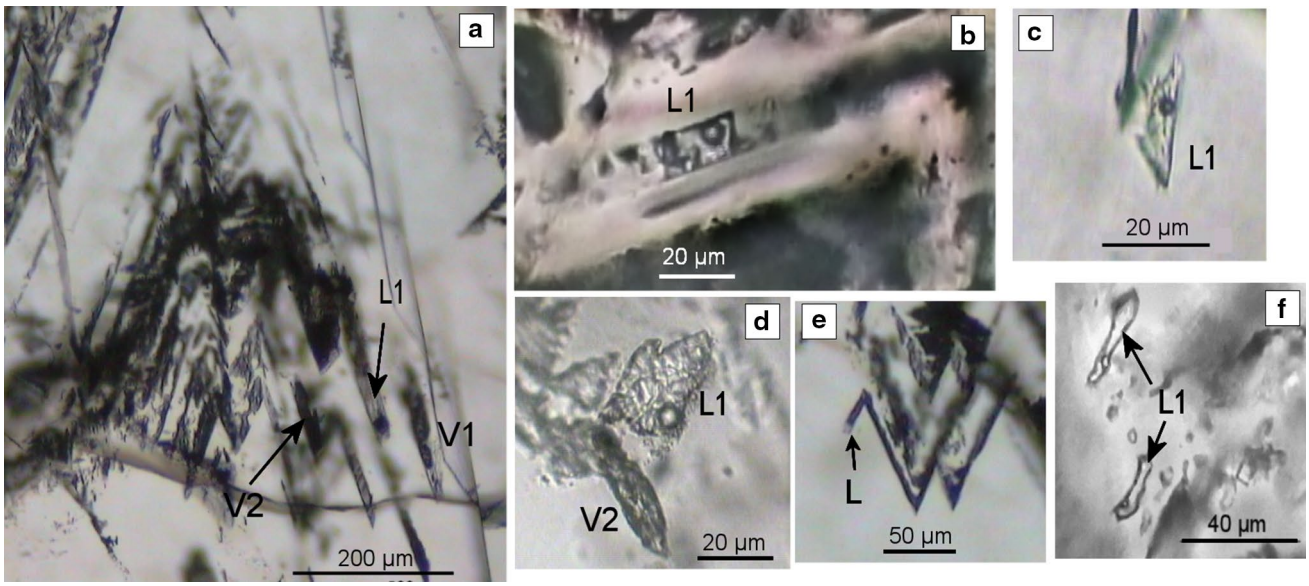

Fig. 9 Photomicrographs (transmitted light, parallel nicols) of fluid inclusions hosted in banded calcite veins of the Castelnuovo dell'Abate travertine; **a** FIA made of liquid-rich (L1), vapour-rich inclusion (V1), and only vapour (V2) in elongated crystals; **b**, **c** examples of L1 inclusions in elongated calcite crystals; **d** coexistence of a liquid-rich (L1) and only vapour (V2) inclusions in elongated calcite; **e** vapour-rich inclusion (V1) with a small portion of liquid; **f** typical FIA of blocky calcites made of two L1 inclusions

Table 2 Summary of the microthermometric data collected for Castelnuovo dell'Abate travertine (L1 type of inclusions)

Sample	Calcite type	Th range (°C)	Tm_{ice} range (°C)
TRS1	Elongated	92.0/136.6 (14)	−0.2/−0.6 (11)
TRS2/1	Elongated	123.8/131.2 (5)	−0.1/−0.7 (6)
	Blocky	90.4/139.5 (35)	0.0/−0.8 (8)
TRS2/2	Elongated	91.6/136.8 (15)	0.0/−0.7 (14)
	Blocky	92.7118.8 (3)	−0.5 (1)

Numbers in brackets refer to the number of fluid inclusions analysed for each sample and calcite type

testify the presence of a vapour phase resulting from fluid immiscibility.

Microthermometric data

The results of microthermometric analyses are summarized in Table 2. To avoid data collection from fluid inclusions affected by necking-down or heterogeneous trapping processes, we discarded the Th of FIA that showed rather variable Th values. Th and Tm_{ice} of single inclusions always fall within the Th and Tm_{ice} ranges of the FIAs; these data

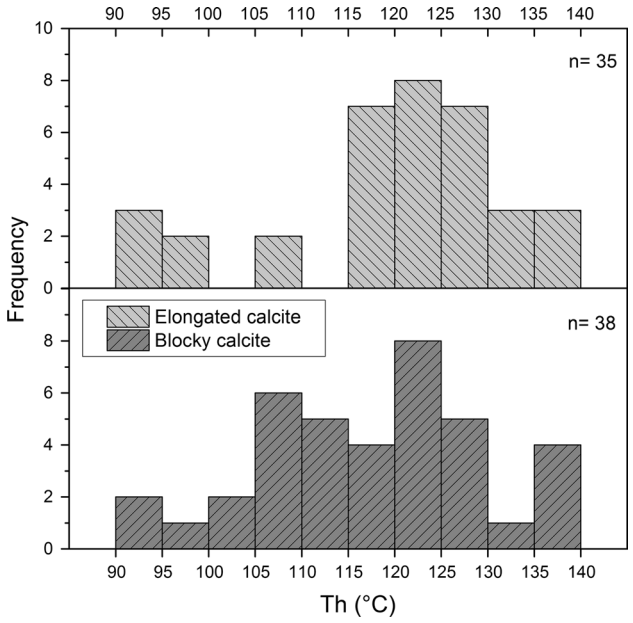

Fig. 10 Results of microthermometry: Th for fluid inclusions hosted in elongated and blocky calcite

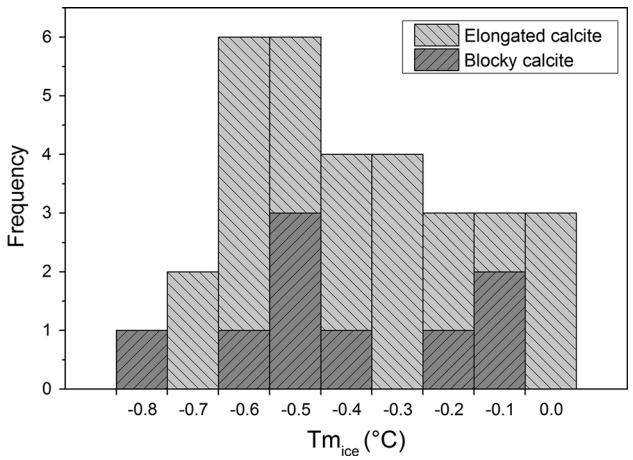

Fig. 11 Results of microthermometry: Tm_{ice} for fluid inclusions hosted in elongated and blocky calcite

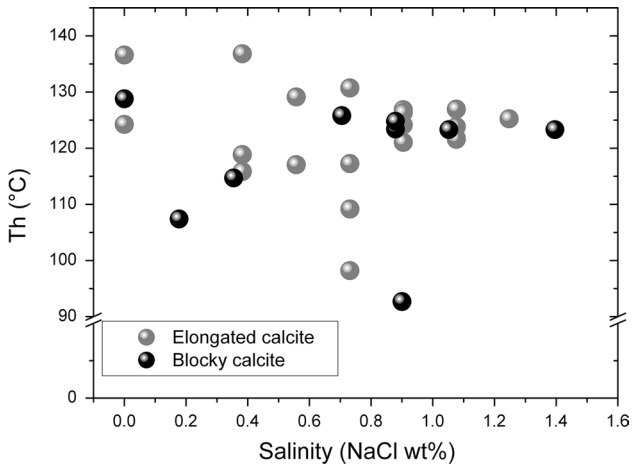

Fig. 12 Th versus salinity for fluid inclusions hosted in elongated and blocky calcite

Table 3 Isotopic composition of the single bands of calcite veins of the Castelnuovo dell'Abate travertine deposit

Sample	$\delta^{13}C$ (PDB)	$\delta^{18}O$ (PDB)	$\delta^{18}O$ (SMOW)
TRS1	0.9	−11.6	19.0
TRS2/1 a	1.1	−11.7	18.8
TRS2/1 b	1.5	−12.4	18.1
TRS2/1 c	0.8	−12.0	18.5
TRS2/2 a	1.4	−10.2	20.4
TRS2/2 b	1.4	−10.7	19.9
TRS2/2 c	1.8	−9.7	20.8
TRS2/2 d	2.2	−11.4	19.1
TRS2/2 e	1.0	−11.8	18.7
TRS3	2.6	−9.5	21.0

TRS2/1a-c and TRS2/2a-e refer to bands microdrilled along the transect of a calcite vein

are reported together with those of the FIAs in the frequency histograms of Figs. 10 and 11. Most FIAs of L1 inclusions showed consistent Th data accordingly to the criteria of Goldstein and Reynolds (1994). Distinct FIAs are usually characterized by different Th ranges. The whole Th range of fluid inclusions, occurring both in elongated and in blocky calcite crystals, is comprised between 90 and 140 °C, with most of values comprised in the 105–140 °C range (Fig. 5).

Th of single L1 inclusions in blocky calcite as well as Th of L1 inclusions in elongated crystals fall within the Th range of L1 inclusions of the FIAs in blocky calcite, suggesting that they trapped similar fluids. Some L2 inclusions nucleate a bubble after freezing; however, the Th measured after bubble nucleation was always higher than the Th of the coexisting L1 inclusions, likely because of stretching process upon ice formation at low temperature. These data were not considered in the following discussion.

Decrepitation phenomena during cooling also reduced the number of L1 fluid inclusions analysed for Tm_{ice} ($n = 40$), which varied from −0.8 to 0.0 °C in both calcite types (Fig. 11), corresponding to salinities of 0–1.4 wt% NaCl eq. Apparent salinities are homogenously distributed among the analysed samples and do not show any clear correlation with Th (Fig. 12). During low-temperature microthermometric analysis, no ice melting was observed within V1 and V2 inclusions.

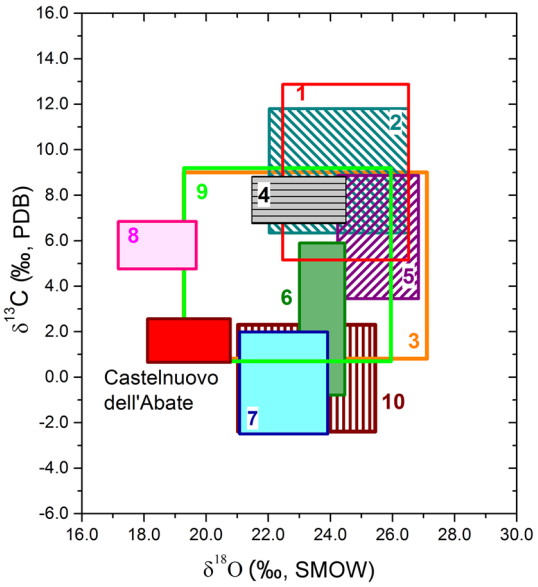

Fig. 13 $\delta^{13}C$-$\delta^{18}O$ composition of Latial and Tuscan travertines compared to the Castelnuovo dell'Abate deposit. Data from Fouke et al. (2000), Fritz (1965), Manfra et al. (1976) and Minissale (2004). Latial travertine—*1* Tivoli, *2* Canino, *3* Viterbo, *4* Cisterna di Latina, *5* Fiano Romano, *6* Ferentino. Tuscan travertine—*7* Sarteano, *8* Bagni San Filippo, *9* Rapolano, *10* Casciana Terme

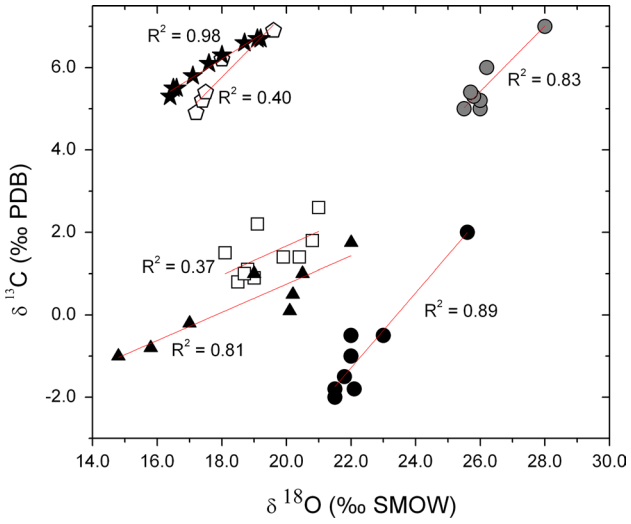

Fig. 14 $\delta^{13}C$–$\delta^{18}O$ correlation in Castelnuovo dell'Abate travertines (this study) and other Tuscan and Latial deposits (data from Minissale et al. 2002; Fouke et al. 2000; Gonfiantini et al. 1968). *Open square* Castelnuovo dell'Abate, *open pentagon* Bagni San Filippo, *grey filled circle* Castelnuovo Berardenga, *filled star* Bagnaccio, *black filled circle* Casciana Terme, *filled triangle* Massa Marittima

Crushing tests

Crushing tests were performed successfully only on small number of L1 inclusions. Upon crushing, few inclusions showed the contraction of the gas bubble, while in the other inclusions the gas bubbles expanded but did not completely fill the cavity of the inclusions. Bubble expansion indicates the presence of pressurized gases (>1 bar) in the bubble. These gases are probably made up mainly of CO_2, as this is the dominant gas in systems depositing travertine. An estimate of CO_2 content was made by using the graphical method of Sasada (1985) based on bubble behaviour during crushing tests. The CO_2 concentration is between 0.07 and 0.14 mol% considering a Th range of 100–140 °C for inclusions showing bubble expansion with incomplete cavity filling. For inclusions exhibiting bubble shrinkage, the CO_2 content is below 0.07 mol%.

Stable isotope composition

Oxygen and carbon isotope data of calcite veins are reported in Table 3. $\delta^{13}C$ showed a consistently positive value for all samples (average value = 1.5 ‰; 2σ = 0.6 %). Along transects, calcite veins showed very small fluctuations in oxygen and carbon composition (Table 3), suggesting minor (isotopic) variations in fluid geochemistry during vein deposition. $\delta^{13}C$ and $\delta^{18}O$ of the Castelnuovo dell'Abate calcite veins are similar to those observed for travertines of central Italy (Fig. 13). At Castelnuovo dell'Abate, $\delta^{18}O$ of calcite is relatively low but comparable to those of the Bagni San Filippo travertine (Minissale 2004).

In contrast to other Italian deposits, the Castelnuovo dell'Abate travertine does not show a clear positive $\delta^{13}C$-$\delta^{18}O$ correlation ($R^2 = 0.37$) (Fig. 14).

U/Th dating

U concentrations in the samples varied between 1.00 and 2.84 mg kg^{-1}, while concentrations of ^{232}Th ranged between 18.07 and 1041 μg kg^{-1} (average of 494.4 ± 1.15 (2σ) μg kg^{-1}) (Table 4). The measured ratio for $^{230}Th/^{232}Th$ varied between 114.55 ± 0.51 and 16.72 ± 0.09 (± 2σ). After non-radiogenic or detrital ^{230}Th correction, the analysed vein samples provided an age range between 368 ± 112 ka and 389 ± 19 ka. Corrected ages of two bands from sample TRS1 were 385 ± 75 ka (TRS1_12) and 368 ± 112 ka (TRS1_20); 389 ± 19 ka for TRS2/1_25, and 370 ± 14 ka for TRS2/2_35 (Table 4). These ages are identical considering the uncertainties due to detrital ^{230}Th correction and define the samples maximum ages. In contrast, sample TRS2/2_90 has a high U content and does not fit the U–Th evolution trend. This implies partial U loss, resulting in excess ^{230}Th unsupported by ^{234}U decay.

Although the calibration method was designed to minimize the error caused by the uncertainty in decay constant for ^{230}Th and ^{234}U, the age of the samples is close to secular equilibrium and therefore strongly affected by error

Table 4 U–Th isotopic data for single calcite bands of Castelnuovo dell'Abate

Sample ID	U (mg kg^{-1})	^{232}Th (μg kg^{-1})	(^{230}Th/^{232}Th)	(^{230}Th/^{238}U)	±2σ	(^{234}U/^{238}U)	±2σ	(^{230}Th/^{238}U) age (ka)	±2σ	Initial (^{234}U/^{238}U)
TRS1_12	2.84	782.0	26.64	2.4221	0.0175	2.0975	0.0060	385	75	4.5273
TRS1_20	2.34	1041	16.72	2.4517	0.0119	2.1346	0.0054	368	112	4.6568
TRS2/1_25	2.10	136.9	114.55	2.4587	0.0102	2.1238	0.0032	389	19	4.4317
TRS2/2_35	1.00	18.07	405.0	2.4110	0.0168	2.1046	0.0040	370	14	4.1615
TRS2/2_90	6.73	36.95	1557.8	2.8170	0.0131	2.1411	0.0043	Unable to calculate		Unable to calculate

TRS1_12, 20 and TRS2/2_35/90 refer to calcite bands drilled along transects

magnification. Another factor complicating the interpretation of the data is the uncertainty in the correction for a possible contribution of non-radiogenic (initial/detrital) ^{232}Th, as the assumed bulk-Earth values may not be applicable to these samples. Irrespective of these limitations, the data seem to suggest that (with the exception of sample TRS2/2_90, which cannot be accurately dated using this method) all the samples formed virtually at the same time at ~370–390 ka.

Discussion

Mineralogy of Castelnuovo dell'Abate travertine deposit

Banded travertine veins are generally composed by almost pure $CaCO_3$, which may occur in the form of calcite or aragonite, depending on numerous factors such as temperature, chemical composition (Mg/Ca ratio; Kele et al. 2011), presence of Sr^{2+} or SO_4^{2-} (Malesani and Vannucci 1975), pCO_2 and CO_2 degassing rate (Kele et al. 2008). It is generally assumed that aragonite forms preferentially at $T > 40$ °C, while calcite dominates in the $T < 30$ °C domain for unstirred solution belonging to the H_2O–CO_2–$CaCO_3$ system (Fouke et al. 2000). Actually, it has been noted, however, that changes in the degree of supersaturation due to CO_2 degassing greatly influence these temperature limits (Chafetz et al. 1991; Renaut and Jones 1997). The rate of precipitation may further control the polymorph being precipitated, with rapid deposition favouring aragonite but not necessarily excluding calcite from the mineral assemblage (Renaut and Jones 1997). More precisely, slow degassing rates under low P_{CO_2} favour calcite precipitation, whereas aragonite is more frequent under high degassing rates and high levels of supersaturation (Arnórsson 1989). The Castelnuovo dell'Abate banded veins are essentially composed of calcite. Aragonite is absent, and there is no evidence of a post-depositional transition from aragonite to calcite. The typical radial texture of calcite observed in the field and the supposed conditions of precipitation (i.e. during fluid immiscibility) are indicative of a high rate of precipitation of the carbonatic phase (Simmons and Christenson 1994). Relatively high levels of Sr in calcite further confirm this hypothesis, since the co-precipitation of elements with distribution coefficient <1, like Sr, is enhanced by high rates of precipitation (Kele et al. 2008).

Low P_{CO_2} during fluid immiscibility might then have been the controlling factor for the deposition of calcite along the Castelnuovo dell'Abate fault, consistent with the relatively low concentrations of dissolved CO_2 observed in fluid inclusions study (see "Mineralogy of Castelnuovo dell'Abate travertine deposit" section). Similar conditions have been documented in Kenya (Renaut and Jones 1997; Renaut et al. 2013) and in New Zealand (Jones et al. 1996), where calcite precipitates directly from waters at temperature higher than 90 °C.

The Castelnuovo dell'Abate banded calcite veins display distinctive mineralogical features, like the presence of fluorite, pyrite and associated high levels of As (Table 1). Travertine is often enriched in volatile and semi-volatile elements, such as F (Pentecost 2005). Fluorite has been documented in Colorado, New Mexico and Kenya travertines (Pentecost 2005; Renaut et al. 2013). Since fluorite shows prograde solubility in the temperature/salinity range suggested by fluid inclusions (Richardson and Holland 1979), fluorite likely followed calcite deposition at Castelnuovo dell'Abate, being related to cooling of the hydrothermal fluid (Renaut et al. 2013) and/or a drop in salinity, following fluid mixing. High levels of F (several mg L^{-1}) are also documented in modern thermal springs of Tuscany and Latium (Minissale et al. 2002; Frondini et al. 2008), and travertine-depositing waters are often oversaturated in fluorite (Di Benedetto et al. 2011). The elevated concentrations of F and Sr in fossil and current travertine deposits suggest deep circulation of waters inside the Tuscan rock pile (Minissale et al. 2002). According to Barbieri et al. (1976), these fluids interact with the Late Triassic evaporite horizon (Burano Fm.) and the Mesozoic carbonate succession, which may be the ultimate source of Sr and F. This

interaction, however, did not yield very saline fluids as testified by the salinity observed in fluid inclusions (maximum salinity = 1.4 wt% NaCl eq.) (see "Calcite vein deposition" section), likely because Triassic evaporites in southern Tuscany are mainly composed by anhydrite (or gypsum), which is not extremely soluble, whereas halite occurs only in minor amounts (De Paola et al. 2008).

Arsenic is frequently reported in thermal springs, although its occurrence in travertines is rarely investigated (Pentecost 2005). Arsenic, however, is an important component in travertine deposits of Western Turkey (Dogan and Dogan 2007), Greece (Winkel et al. 2013) and Italy (Dessau 1968; Di Benedetto et al. 2006; Costagliola et al. 2013). The association between travertine and As in southern Tuscany and northern Latium is well documented, and up to hundreds mg kg^{-1} of As is found in fossil travertine and calcareous tufa deposits (Costagliola et al. 2010, 2013; Di Benedetto et al. 2011). At Castelnuovo dell'Abate, As is mainly associated with primary pyrite (and pseudomorph Fe-(hydr)oxides after pyrite), which possibly scavenged the metalloid from the hydrothermal fluids.

Calcite vein deposition

Temperature and salinity of the fluid that formed the Castelnuovo dell'Abate banded travertine can be obtained from the fluid inclusion data. Fluid inclusions petrography indicates that several inclusions formed during fluid immiscibility, consequently, Th of such inclusions corresponds to the trapping temperature (e.g. Shepherd et al. 1985). Moreover, considering the shallow environment of travertine formation characterized by fluid pressure not exceeding few tens of bars (see later in this paragraph), pressure correction to be added to Th to obtain the trapping temperature is insignificant, and Th values of all L1 inclusions can be considered representative of the trapping temperatures.

As different FIAs are often characterized by distinct Th ranges, temperature fluctuations probably occurred during calcite deposition. Such fluctuation may have produced thermal re-equilibration of some fluid inclusions, specifically of those occurring in the few FIAs that showed not consistent data accordingly to the criteria of Goldstein and Reynolds (1994) and possibly of single large fluid inclusions. Moreover, because of the scarce and random distribution of fluid inclusions in calcite, microthermometric data do not allow specific characterization of temperature and salinity for different calcite generations but provide general information during calcite precipitation. Therefore, as fluid inclusions homogenized between 90 and 140 °C, the temperature of calcite forming solution was at least within this range.

According to field observations, the Castelnuovo dell'Abate banded travertine occurs as multiple generations of banded calcite veins, which propagated from a feeding channel localized along a tract of the Castelnuovo dell'Abate fault. The fault acted as a preferential conduit for the ascending Ca-rich fluids, which came to the surface precipitating travertine. Accordingly, thermal springs occurring in southern Tuscany and in other geothermal fields elsewhere mainly relate to extensional structures (Kerrich 1986; Hancock et al. 1999; Brogi and Capezzuoli 2009), enhancing the genetic link between travertine deposition and recent tectonics. The local occurrence of wall rock fragments in the banded calcite veins suggests that travertine deposition was accompanied by the injection of overpressured fluids, probably associated with a hydrothermal eruption (cf., Hedenquist and Henley 1985) and hydrofracturing (Gudmundsson et al. 2002; Uysal et al. 2009; Buttinelli et al. 2011). Recent episodes of fossil and present-day hydrofracturing are documented in the nearby Larderello geothermal area, in the form of phreatic craters and explosions (Marinelli 1969), driven by high-pressure fluids (Ruggieri and Gianelli 1999; Gianelli 2008).

The above-mentioned features as well as the banded vein texture suggest a rhythmical precipitation of calcite caused by cyclic events that can be schematized in five steps: (a) light depressurization of the hydrothermal system by hydraulic fracturing, possibly triggered by tectonic activity; (b) immiscibility of a liquid and vapour phase for adiabatic decompression (Fournier 1985); (c) ascent of the fluid in the near-vertical channel; (d) CO_2 degassing and associated calcite (and then travertine) deposition by the reaction $Ca(HCO_3)_2 \rightarrow CaCO_3 + CO_2\,(\uparrow) + H_2O$ (Brasier 2011); and (e) sealing of the conduits that reduced the rock permeability and prepared the system for a new cycle. Under this scenario, the multiple calcite generation as well as their banded fabric is indicative of a travertine multistage deposition.

The relative wide range of variability of apparent salinities in fluid inclusions (0.0–1.4 wt% NaCl eq.) might provide further information on the chemical composition of the parent fluid. However, the possible presence of dissolved CO_2 in fluid inclusions should be considered, as this may depress the Tm_{ice} and thus result in an overestimation of the real salinity (Hedenquist and Henley 1985). In L1 inclusions, the range of CO_2 varies between 0 mol% (inclusions displaying Tm_{ice} of 0.0 °C), suggesting that they represent almost pure water, and 0.14 mol%, as indicated by the crushing tests. The variable amount of CO_2 can be easily explained considering the cyclic evolution of the systems precipitating calcite: the self-sealing process produces the closing of the system towards the surface and the increase in pressure above hydrostatic conditions, causing the system to reach its maximum CO_2 content. The maximum pressure reached in the system can be evaluated from the Duan and Sun (2003) CO_2 solubility data, assuming that the maximum CO_2 content was reached when the

fluid was at 140 °C with a salinity of about 1.4 wt% NaCl eq. (the maximum value of salinity observed). Under these conditions, the fluid pressure was ~13 bars. Hydraulic fracturing led then to depressurization and, consequently, to fluid immiscibility with CO_2 degassing. The occurrence of fluid inclusions that homogenize below 100 °C is further compatible with a hydrothermal solution encompassing cyclic cooling (due to boiling) followed by a new heating and eventually a new heterogeneous trapping.

The highest CO_2 content in the trapped fluid (0.14 mol%) gives a Tm_{ice} depression of 0.15 °C, corresponding to a maximum overestimation of the salinity computed from Tm_{ice} of 0.27 wt% NaCl eq. Thus, the salinity range showed by L1 inclusions can be only marginally ascribed to changes in the CO_2 content of the fluid. Different salinities in fluid inclusions may be indicative of one or more of these three processes occurring during trapping: (1) mixing of two fluids, characterized by different salinities but comparable temperatures; (2) condensation of the low-salinity vapour resulting from fluid immiscibility processes; and (3) immiscibility taking place under disequilibrium conditions for CO_2.

The depth of the Castelnuovo dell'Abate system can be estimated assuming that the maximum pressure of the fluid (13 bars) corresponds to the pressure necessary to produce hydrofracturing. In extensional tectonic regimes, such as in southern Tuscany, the following relation proposed by Hubbert and Willis (1957) may apply:

$$P_{\text{hydrofracturing}} \cong \frac{(P_{\text{lithostatic}} + 2P_{\text{hydrostatic}})}{3}$$

Since the $P_{\text{lithostatic}}$ is approximately 2.5 times the $P_{\text{hydrostatic}}$, $P_{\text{hydrostatic}}$ was estimated to be about 9 bars corresponding to a depth of travertine formation of about 75 m. Such a depth is in agreement with the difference in altitude between the roof of bedded travertine and the base of banded veins, also considering the erosion that the surface deposit has undergone in 350–400 ka.

Isotopic composition and age

The $^{13}C/^{12}C$ and $^{18}O/^{16}O$ isotopic ratios of Castelnuovo dell'Abate calcite banded veins are in the low range of those observed for hot-spring travertines of central Italy (Fig. 13), and similar to the isotopic ratios commonly observed for thermal-derived deposits (Pentecost 2005; Turi 1986).

Stable C and O isotopes have proved to be a suitable tool to understand the genesis of travertine (Friedman 1970; Manfra et al. 1976; Turi 1986), and the provenance of its source fluid (Minissale et al. 2002). Theoretically, information on the fractionation factors in the CO_2–$CaCO_3$–H_2O system allows to the calculation of the $\delta^{18}O$ and $\delta^{13}C$ of the parent solution from the measurable ratios in fossil travertine. Isotopic equilibrium, however, is rarely attained during travertine deposition (Gonfiantini et al. 1968; Friedman 1970), since kinetic effects (fluid degassing and evaporation, microbial activity) and diagenesis are highly effective in causing appreciable shifts from the theoretically expected isotope composition (Friedman 1970; Kele et al. 2008; Manfra et al. 1974; Minissale et al. 2002; Pentecost 2005).

For C, fractionation occurs mainly during CO_2 degassing, resulting in loss of light ^{12}C and consequent increase of $\delta^{13}C$ in the deposited rock (Guo et al. 1996). In contrast, CO_2 degassing does not significantly affect $\delta^{18}O$ of dissolved C compounds, which are generally buffered trough rapid re-equilibration by the O isotope composition of the water (Zheng 1990). Oxygen composition, however, is in turn influenced by the preferential evaporation of $H_2^{16}O$ (Turi 1986). Consequently, downstream of the spring, travertines progressively become enriched in ^{18}O and ^{13}C, displaying a linear positive $\delta^{18}O$–$\delta^{13}C$ correlation (Gonfiantini et al. 1968; Kele et al. 2008). This trend can be expected to be quite strong for surface (open air) travertine precipitation (e.g. cascades or lacustrine facies), but relatively weak precipitation along veins, such as Castelnuovo dell'Abate banded travertine. Here, the absence of a clear positive $\delta^{18}O$–$\delta^{13}C$ correlation (Fig. 14) (Vermoere et al. 1999) and the fairly constant C–O isotope composition of calcite (Table 3) suggest that: (a) the isotopic composition of waters remained constant during travertine deposition, and (possibly) travertine precipitated under isotopic equilibrium, or (b) a number of factors (*T*, isotopic composition of the fluid, Rayleigh distillation processes, etc.) varied in the same way, resulting in negligible changes in the $\delta^{18}O$–$\delta^{13}C$ systematics.

Assuming equilibrium conditions between fluid and calcite, the $\delta^{18}O$ composition of the parent fluid was determined by the equation of Friedman and O'Neil (1977), supposing that most of calcite deposition had occurred in a temperature range of 100–140 °C (Fig. 10). The resulting $\delta^{18}O$ of the hydrothermal water ranges from +0.9 to +7.4 ‰ (Fig. 15) and is strongly enriched in ^{18}O with respect to the present-day regional rainwater ($\delta^{18}O = -7.0$ to −6.0 ‰; Fig. 15; Longinelli and Selmo 2003), which is believed to feed the shallow hydrothermal systems of southern Tuscany (Minissale et al. 1997; Minissale 2004). Even though some isotopic shift due to disequilibrium is conceivable, a strictly meteoric composition for the travertine fossil fluid is unrealistic. The O composition of a hypothetical calcite deposited in a temperature range of 100–140 °C from a typical meteoric fluid ($\delta^{18}O = -7.0$ ‰) would have resulted in $\delta^{18}O$ ranging from 6 to 10 ‰. Therefore, to account for the $\delta^{18}O$ values measured in Castelnuovo dell'Abate calcites ($\delta^{18}O = +18.1$ to +21 ‰), an isotopic shift of more than 10 ‰ should be assumed, which is much

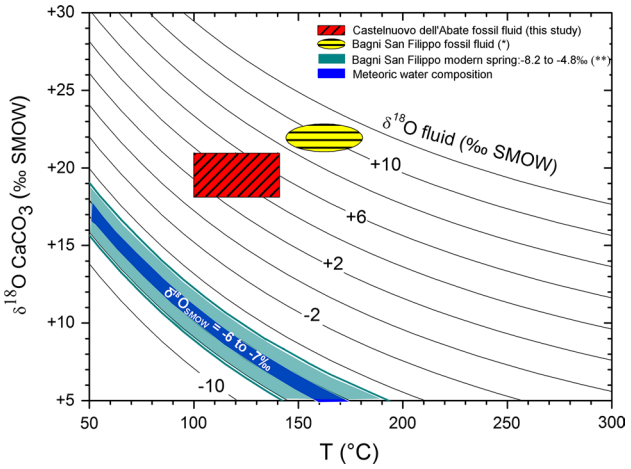

Fig. 15 Homogenization temperatures versus $\delta^{18}O$ for the banded calcite veins of Castelnuovo dell'Abate. The $\delta^{18}O$ composition of the fluid in equilibrium with calcite was calculated using the fractionation equation of Friedman and O'Neil (1977), in the 100–140 °C Th range. The composition of Bagni San Filippo modern and fossil thermal springs and of rainwater of southern Tuscany is reported. *Data from Gasparrini et al. (2013); **from Fancelli and Nuti (1975), DST (2010)

higher than that observed for deposits formed on the surface under disequilibrium conditions (Kele et al. 2008, 2011). The simplified assumption of travertine deposition under equilibrium conditions is believed then to be valid, at least to indicate that the Castelnuovo dell'Abate fossil fluid was enriched in ^{18}O (likely caused by water–rock interaction processes, see "Present and fossil hydrothermal systems of southern Tuscany" section) with respect to the present-day regional rainwater.

Carbon isotopic composition of CO_2 ($\delta^{13}C_{CO_2}$) was calculated using the equation of Bottinga (1969), which directly relates the $\delta^{13}C$ of fossil deposits ($\delta^{13}C_{CaCO_3}$) to $\delta^{13}C_{CO_2}$. Additionally, $\delta^{13}C_{CO_2}$ was derived using the empirical equation of Panichi and Tongiorgi (1976) ($\delta^{13}C_{CO_2} = 1.2\ \delta^{13}C_{CaCO_3}$—10.5), obtained specifically for Italian travertine.

For the assumed temperature range of deposition (100–140 °C), the calculated $\delta^{13}C_{CO_2}$ ranged from −3.2 to +1.2 ‰ (Bottinga 1969) and from −9.5 to −7.4 ‰ (Panichi and Tongiorgi 1976), respectively. The composition derived from Panichi and Tongiorgi (1976) is then markedly more negative than that determined by the Bottinga's equation. Such large difference is probably related to the different conditions that apply to the two equations: the Bottinga (1969) equation requires equilibrium conditions, whereas the empirical relationship of Panichi and Tongiorgi (1976) was obtained for travertine deposited in surface environments characterized by large and rapid degassing processes which strongly affect $\delta^{13}C_{CO_2}$. Bottinga's equation appears then to be appropriate to calculate the $\delta^{13}C_{CO_2}$ of Castelnuovo dell'Abate fluids since this banded travertine formed under hypogenetic conditions, and significant degassing occurred only during hydraulic fracturing events and consequent depressurization. Moreover, the $\delta^{13}C_{CO_2}$ of the nearby travertine deposits of Bagni San Filippo and Bagno Vignoni (−6.1 to −2.0 ‰; Fig. 1), calculated using the Panichi and Tongiorgi (1976) equation from $\delta^{13}C_{CaCO_3}$ (+3.4 to +6.8 ‰; Minissale 2004), is systematically higher than those calculated for the Castelnuovo dell'Abate system with the same equation, whereas the $\delta^{13}C_{CO_2}$ values of the three sites partially overlap when calculated using the Bottinga (1969) equation. Thus, even if the assumption of travertine deposition under equilibrium conditions may be not totally respected, the $\delta^{13}C_{CO_2}$ range obtained from Bottinga (1969) is to some extent similar to the $\delta^{13}C_{CO_2}$ range (−4.6 to −2.3 ‰; Minissale 2004; Frondini et al. 2009) of the present-day CO_2-rich gas emissions occurring in the area surrounding Castelnuovo dell'Abate. The CO_2 in these emissions and more in general in the emissions of the Monte Amiata area is believed to result from a mixture of different sources such as mantle degassing and thermometamorphic (decarbonation) reactions (Minissale 2004; Frondini et al. 2009; Tassi et al. 2009). A similar composite origin can be proposed also for the CO_2 of the Castelnuovo dell'Abate, although the more positive $\delta^{13}C_{CO_2}$ values displayed by this system suggest a larger contribution from decarbonation reaction and/or ^{13}C enrichment due to degassing as a consequence of hydraulic fracturing events.

The widespread and sustained hydrothermal activity in the Monte Amiata area is commonly related to magmatism, whose volcanic products have radiometric ages of 300–200 ka, based on K/Ar (Bigazzi et al. 1981; Cadoux and Pinti 2009) and $^{40}Ar/^{39}Ar$ (Laurenzi and Villa 1991; Barberi et al. 1994) dating of sanidine and plagioclase, and fission tracks on volcanic glass (Bigazzi et al. 1981). To date, the only available age data for the hydrothermal circulation related to the Monte Amiata thermal anomaly is the $^{230}Th/^{234}Th$ age of some lacustrine deposits (diatomites) (Fornaca Rinaldi 1968). The 370–390 ka age data obtained for calcite in this study provide clear evidence that the hydrothermal systems were already established before the Monte Amiata volcanic manifestations, suggesting that the thermal anomaly at Monte Amiata predated volcanism. This observation agrees with the model proposed by Cadoux and Pinti (2009), which suggests a long-pre-eruptive evolution of the magma chamber of the Monte Amiata volcano. According to this model, the thermal anomaly developed in response to the emplacement of a large magma body in the upper crust. Such intrusion probably corresponds to the large uplifted region in the Monte Amiata area, showing an elliptical shape with major axes of 25–30 and 45–50 km (Gianelli et al. 1988). Ages up to 218 ka have been reported for the travertine plate of Montemerano (Fig. 1; Taddeucci

and Voltaggio 1987), and the stratigraphic age of the nearby Semproniano travertine (Fig. 1) has been assigned to the Lower Pliocene (Bosi et al. 1996). These deposits further document the presence of a thermal anomaly that predates the Monte Amiata volcanism.

As suggested by this study, at least part of the CO_2 of the shallow hydrothermal system at Castelnuovo dell'Abate had a deep source, whereas the low salinities of fluid inclusions exclude a direct input of magmatic-derived water in the system. It is conceivable that the effect of the magma emplacement at Monte Amiata was limited to the influx of deep CO_2 and to the activation of a hydrothermal circulation, which was in turn fed by meteoric waters.

Present and fossil hydrothermal systems of southern Tuscany

Abundance of hot springs, CO_2-dominated gas emissions, travertine-depositing manifestations and the widespread occurrence of CO_2 in present-day geothermal fields provide clear evidence for active CO_2-rich hydrothermal systems occurring in southern Tuscany (Minissale et al. 1997). Bagni San Filippo is one of the best characterized examples of long-lived (since the Pleistocene) CO_2-rich hydrothermal systems in the region, as suggested by the presence of an exhumed Hg mineralization with Pleistocene age. The water currently discharged by this system, depositing travertine on the surface, is characterized by TDS of 4128 mg/l and a temperature of 52 °C (Minissale 2004). Equilibrium temperatures of the aquifer feeding the surface system are comprised in the 60–95 °C range, whereas pCO_2 value estimated at 60 °C is about 10 bar (Donnini et al. 2007, Baietto et al. 2008).

In the following discussion, the travertine deposit associated with the thermal spring of Bagni San Filippo (and Bagno Vignoni) will be considered as a modern analogue of the Castelnuovo dell'Abate system since these localities are located within a radius of few kilometres of distance and share some common geological and geochemical features. Hydrothermal circulation at these sites was favoured by the presence of Neogene-Quaternary brittle structures (Brogi et al. 2010a, b, 2012) that allowed the upwelling of large volumes of meteoric-derived aqueous solutions, heated by the regional high geothermal gradient and enriched in Sr and F through their circulation in Mesozoic carbonate and Triassic evaporite successions (e.g. host rocks of the shallower reservoir; Duchi et al. 1992; Cortecci and Lupi 1994; Gasparrini et al. 2013; Brogi et al. 2015).

Following the data of Gasparrini et al. (2013) on hydrothermal calcite veins sampled in Mesozoic carbonate rocks of the Monte Amiata surroundings, the Bagni San Filippo fossil hydrothermal system was characterized by temperatures of about 165 °C, relatively low salinities (generally comprised between 1.2 and 1.7 wt% NaCl eq.), $\delta^{13}C = -2.6$ to $+0.6$ ‰ and $\delta^{18}O = +21.6$ to $+23.1$ ‰ (Gasparrini et al. 2013) (Fig. 10). These isotopic values are similar to those observed in the Castelnuovo dell'Abate fossil system (Table 3), further highlighting the similarities between these two systems.

The present-day hydrothermal system of Bagni San Filippo shows a lighter isotopic composition of water with $\delta^{18}O$ between –8.2 ‰ and –4.8 ‰ (Gonfiantini et al. 1968; Fancelli and Nuti 1975; DST 2010; Fig. 15), thus markedly different from the (calculated) much heavier O isotope composition of the water that fed the same system in the past ($\delta^{18}O = +8.4$ to $+11.6$ ‰; Gasparrini et al. 2013) and from the water that deposited the Castelnuovo dell'Abate travertine ($\delta^{18}O = +0.9$ to $+7.4$ ‰; this study). Accordingly, hydrothermal calcite veins developed around the geothermal anomalies of southern Tuscany generally indicate an O composition in fossil fluids heavier than meteoric water (Liotta et al. 2009). Concerning the Castelnuovo dell'Abate and Bagni San Filippo fossil hydrothermal systems, inputs of heavy O isotopes from a magmatic source water could be reasonably excluded based on the low salinities of the fluid inclusions in calcite, which suggest a meteoric origin of the original waters feeding the Castelnuovo dell'Abate system. In contrast, it could be argued that in fossil hydrothermal systems, the meteoric waters interacted, more extensively than today, with the rocks belonging to the Tuscan Nappe rock pile (Cortecci and Lupi 1994; Gasparrini et al. 2013) and relatively enriched in ^{18}O. The O isotopic signatures of calcite of the Tuscan succession are markedly positive ($\delta^{18}O \sim +25$ ‰), with values as high as +28.9 ‰ for the Jurassic limestone (Calcare Massiccio; Fig. 2) (Cortecci and Lupi 1994). This feature marks a clear difference between the fossil and the modern surficial hydrothermal system at least in the Castelnuovo dell'Abate-Bagni San Filippo area. ^{18}O enrichment by water–rock interaction, however, is evident from the isotopic composition ($\delta^{18}O = -3$ to $+1.8$ ‰, DST 2010) of the fluid produced from the shallow reservoir hosted in carbonate rocks of the Monte Amiata geothermal field.

According to fluid inclusions data on hydrothermal calcite veins (Gasparrini et al. 2013), the fluid reservoir of Bagni San Filippo experienced a cooling of about 70–105 °C from vein formation (Pleistocene) to modern time. A similar trend has been observed in the deep Larderello geothermal reservoir, which underwent to a temperature decrease of about 120 °C in the last 3 Ma (Del Moro et al. 1982). Assuming that the Castelnuovo dell'Abate system had the same temperature of the Bagni San Filippo travertine-depositing spring (~50 °C) when it was active, and taking into account the calcite ages, it

can be concluded that the hydrothermal fluids cooled by ~70 °C in 300–400 ka, corresponding to a cooling rate of about 20 °C/100 ka.

Conclusions

The fossil hydrothermal system of Castelnuovo dell'Abate records part of the evolution of the long-lived Monte Amiata geothermal anomaly and has been active for at least the last 400 ka, therefore predating volcanic activity (300–190 ka). The fluids responsible for the deposition of the travertine were characterized using fluid inclusions and stable isotope analysis, and it could be demonstrated that these fluids are compositionally similar to nearby modern depositing travertine springs. This study then clearly suggests that hydrothermal circulation in the Monte Amiata area has undergone moderate changes through time. Accordingly, brittle structures (faults) still trigger the circulation of meteoric-derived, low saline hydrothermal fluids, which interact at depth with a carbonate reservoir. The main differences between past and modern circulation are as follows: (1) the higher temperature reported for the past hydrothermal fluids, which indicates a progressive cooling of surface geothermal systems in the Monte Amiata area in the last 300–400 ka, with a cooling rate that can be estimated at 20 °C/100 ka; and 2) the heavier O isotopic signature of the fossil hydrothermal fluids, indicative of less efficient interaction between the fluids and the host rock in the present-day.

Acknowledgments This study was financially supported by MIUR PRIN 2010–2011 to P. Costagliola and P. Lattanzi. This research was accomplished thanks to the scientific instruments provided by the Ente Cassa di Risparmio di Firenze to the Dipartimento di Scienze della Terra (Università di Firenze). Radiometric age data were obtained using funds provided by the Australian National Centre for Groundwater Research and Training (Program 3). Elena Pecchioni and Mario Paolieri (Università di Firenze) are also gratefully thanked for their assistance during XRD and SEM–EDS analysis. Two anonymous reviewers are also thanked for their help to improve the manuscript.

References

Altunel E, Hancock PL (1993) Morphology and structural setting of Quaternary travertines at Pamukkale, Turkey. Geol J 28:335–346

Altunel E, Karabacak V (2005) Determination of horizontal extension from fissure-ridge travertines: a case study from the Denizli Basin, southwestern Turkey. Geodin Acta 18:333–342

Arnórsson S (1989) Deposition of calcium carbonate minerals from geothermal waters—theoretical considerations. Geothermics 18:33–39

Baietto A, Giudetti G, Governi S, Fusani L, Salvatici E (2008) Shallow versus deep thermal circulations at Bagni di S. Filippo (Mt. Amiata, Tuscany, Italy). 70th EAGE conference and exhibition—workshops and fieldtrips. 9–12 June 2008, Rome. doi:10.3997/2214-4609.201405054

Barberi F, Buonasorte G, Cioni R, Fiordelisi A, Foresi L, Laccarino S, Laurenzi MA, Sbrana A, Vernia L, Villa IM (1994) Plio-Pleistocene geological evolution of the geothermal area of Tuscany and Latium. Mem Descr Carta Geol Ital 49:77–134

Barbieri M, Masi U, Tolomeo L (1976) Distribuzione dello stronzio nei gessi e nelle anidriti delle formazioni evaporitiche dell'Italia centrale. Rend. Soc. Ital. Mineral. Petrol. 32:551–560

Bartole R (1995) The North Tyrrhenian-Northern Apennines post-collisional system: constraints for a geodynamic model. Terra Nova 7:7–30

Batini F, Brogi A, Lazzarotto A, Liotta D, Pandeli E (2003) Geological features of Larderello-Travale and Mt. Amiata geothermal areas (southern Tuscany, Italy). Episodes 26:239–244

Bertini G, Cappetti G, Dini I, Lovari F (1995) Deep drilling results and updating of geothermal knowledge of the Monte Amiata area. In: Proceedings of the world geothermal congress 1995, Florence, pp 1283–1286

Bigazzi G, Giuliani O, Bonadonna FP, Ghezzo C, Radicati Di Brozolo F, Rita F (1981) Geochronological study of the Monte Amiata Lavas (Central Italy). Bull Volcanol 44:455–465

Bodnar RJ, Vytik MO (1994) Interpretation of microthermometric data for H_2O–NaCl fluid inclusions. In: Vivo BD, Frezotti ML (eds) Fluid inclusions in minerals: methods and applications. Virginia Polytechnic Institute, Blacksburg, pp 117–130

Bosi C, Messina P, Rosati M, Sposato A (1996) Età dei travertini della Toscana meridionale e relative implicazioni tettoniche. Mem Soc Geol It 51:239–304

Bottinga Y (1969) Calculated fractionation factors for carbon and hydrogen isotope exchange in the system calcite–carbon dioxide–calcite–methane–hydrogen–water-vapour. Geochim Cosmochim Acta 33:49–64

Brasier AT (2011) Searching for travertines, calcretes and speleothems in deep time: processes, appearances, predictions and the impact of plants. Earth Sci Rev 104:213–239

Brogi A (2008) The structure of the Monte Amiata volcano geothermal area (Northern Apennines, Italy): Neogene–Quaternary compression versus extensions. Int J Earth Sci (Geol Rundsch) 97:677–703

Brogi A, Capezzuoli E (2009) Travertine deposition and faulting: the fault-related travertine fissure-ridge at Terme S. Giovanni, Rapolano Terme (Italy). Int J Earth Sci (Geol Rundsch) 98:931–947

Brogi A, Lazzarotto A, Liotta D, Ranalli G (2005) Crustal structures in the geothermal areas of southern Tuscany (Italy): insights from the CROP 18 deep seismic reflection lines. J Volcanol Geoth Res 148:60–80

Brogi A, Capezzuoli E, Aqué R, Branca M, Voltaggio M (2010a) Studying travertines for neotectonics investigations: Middle–LatePleistocene syn-tectonic travertine deposition at Serre di Rapolano (Northern Apennines, Italy). Int J Earth Sci (Geol Rundsch) 99:1383–1398

Brogi A, Liotta D, Meccheri M, Fabbrini L (2010b) Transtensional shear zones controlling volcanic eruptions: the Middle Pleistocene Monte Amiata volcano (inner Northern Apennines, Italy). Terra Nova 22:137–146

Brogi A, Capezzuoli E, Buracchi E, Branca M, Voltaggio M (2012) Tectonic control on travertine and calcareous tufa deposition in a low-temperature geothermal system (Sarteano, Central Italy). J Geol Soc 169:461–476

Brogi A, Capezzuoli E, Martini I, Picozzi M, Sandrelli F (2014) Late Quaternary tectonics in the inner Northern Apennines (Siena Basin, southern Tuscany, Italy) and their seismotectonic implication. J Geodyn 76:25–45

Brogi A, Liotta D, Ruggieri G, Capezzuoli E, Meccheri M, Dini A (2015) An overview on the characteristics of geothermal carbonate reservoirs in southern Tuscany. It J Geosc. doi:10.3301/IJG.2014.41

Brunet C, Monie P, Jolivet L, Cadet JP (2000) Migration of compression and extension in the Tyrrhenian sea, insights from $^{40}Ar/^{39}Ar$ ages on micas along a transect from Corsica to Tuscany. Tectonophysics 32:127–155

Buttinelli M, De Rita D, Cremisini C, Cimarelli C (2011) Deep explosive focal depths during maar forming magmatic hydrothermal eruption: Baccano Crater, Central Italy. Bull Volcanol 73:899–915

Cadoux A, Pinti DL (2009) Hybrid character and pre-eruptive events of Mt Amiata volcano (Italy) inferred from geochronological, petro-geochemical and isotopic data. J Volcanol Geoth Res 179:169–190

Capezzuoli E, Brogi A, Ricci M, Bertini A (2011) Travertine and calcareous tufa in southern Tuscany (Central Italy). Field Trip Guide book of ISTT (International school of travertine and tufa). Ed. Il Campano, Pisa, p 66

Capezzuoli E, Gandin A, Pedley M (2014) Decoding tufa and travertine (fresh water carbonates) in the sedimentary record: the state of the art. Sedimentology 61:1–21

Carmignani L, Decandia FA, Disperati L, Fantozzi PL, Lazzarotto A, Liotta D, Meccheri M (1994) Tertiary extensional tectonics in Tuscany (Northern Apennines, Italy). Tectonophysics 238:295–315

Carmignani L, Decandia FA, Disperati L, Fantozzi PL, Lazzarotto A, Liotta D, Oggiano G (1995) Relationships between the Sardinia-Corsica-Provençal domain and the northern Apennines. Terranova 7:128–137

Chafetz HS, Rush PF, Utech NM (1991) Microenvironmental controls on mineralogy and habit of $CaCO_3$ precipitates: an example from an active travertine system. Sedimentology 38:107–126

Cheng H, Edwards RL, Hoff J, Gallup CD, Richards DA, Asmerom Y (2000) The half-lives of uranium-234 and thorium-230. Chem Geol 169:17–33

Clark TR, Zhao J-X, Feng Y-X, Done TJ et al (2012) Spatial variability of initial $^{230}Th/^{232}Th$ in modern Porites from the inshore region of the Great Barrier Reef. Geochim Cosmochim Acta 78:99–118

Cortecci G, Lupi L (1994) Carbon, oxygen and strontium isotope geochemistry of carbonates rocks from the Tuscan Nappe, Italy. Mineral Petrol Acta 37:63–80

Costagliola P, Benvenuti MM, Benvenuti MG, Di Benedetto F, Lattanzi P (2010) Quaternary sediment geochemistry as a proxy for toxic element source: a case study of arsenic in the Pecora Valley (southern Tuscany, Italy). Chem Geol 270:80–89

Costagliola P, Bardelli F, Benvenuti M, Di Bendetto F, Romanelli M, Paolieri M, Rimondi V, Vaggelli G (2013) Arsenic bearing-calcite in natural travertines: evidence from sequential extraction, μ-XAS and μ-XRF. Environ Sci Technol 47:6231–6238

Craig H (1957) Isotopic standards for carbon and oxygen and correction factors for mass-spectrometric analysis of carbon dioxide. Geochim Cosmochim Acta 12:133–149

De Filippis L, Faccenna C, Billi A, Anzalone E, Brilli M, Soligo M, Tuccimei P (2013) Plateau versus fissure ridge travertines from Quaternary geothermal springs of Italy and Turkey: interactions and feedbacks between fluid discharge, paleoclimate, and tectonics. Earth-Sci Rev 123:35–52

De Paola N, Collettini C, Faulkner DR, Trippetta F (2008) Fault zone architecture and deformation processes within evaporitic rocks in the upper crust. Tectonics 47:TC4017

Del Moro A, Puxeddu M, Radicati di Bronzolo F, Villa IM (1982) Rb-Sr and K-Ar ages on minerals at temperatures of 3000–400°C from deep wells in the Larderello geothermal field (Italy). Contrib Mineral Petrol 81:340–349

Della Vedova B, Bellani S, Pellis G, Squarci P (2001) Deep temperatures and surface heat flow distribution. In: Vai GB, Martini IP (eds) Anatomy of an orogen: the Apennines and adjacent Mediterranean basins. Kluwer, Dordrecht, pp 65–76

Dessau G (1968) Il berillio e l'arsenico nei travertini dell'Italia Centrale. Atti Soc Tosc Sci Nat 75:690–711

Di Benedetto F, Costagliola P, Benvenuti M, Lattanzi P, Romanelli M, Tanelli G (2006) Arsenic incorporation in natural calcite lattice: evidence from electron spin echo spectroscopy. Earth Planet Sc Lett 246:458–465

Di Benedetto F, Montegrossi G, Minissale A, Pardi LA, Romanelli M, Tassi F, Delgado Huertas A, Pampin EM, Vaselli O, Borrini D (2011) Biotic and inorganic control on travertine deposition at Bullicame 3 spring (Viterbo, Italy): a multidisciplinary approach. Geochim Cosmochim Acta 75:4441–4455

Diamond LW (2003) Systematics of H_2O inclusions. In: Samson IM, Anderson AJ, Marshall DD (eds) Fluid inclusions: analysis and interpretation. Mineralogical Association of Canada, Short Course 32, pp 55–80

Dini A, Gianelli G, Puxeddu M, Ruggieri G (2005) Origin and evolution of Pliocene–Pleistocene granites from the Larderello geothermal field (Tuscan Magmatic Province Italy). Lithos 81:1–31

Dogan M, Dogan AU (2007) Arsenic mineralization, source, distribution, and abundance in the Kutahya region of the western Anatolia, Turkey. Environ Geochem Health 29:119–129

Donnini M, Chiodini G, Avino R, Baldini A, Cardellini C, Caliro S, Frondini F, Granieri D, Morgantini N (2007) Carbon dioxide degassing at Bagni san Filippo (Tuscany, Italy): quantification and modelling of gas release. Geophys Res Abstr 9, EGU2007-A-02954

DST-Dipartimento di Scienze della Terra Università di Firenze - Gruppo di Geochimica (2010) Indagine geochimica ed isotopica delle sorgenti termo- ed oligominerali dell'area amiatina. Regione Toscana. Accordo di Programma Quadro Ricerca e trasferimento tecnologico per il sistema produttivo, 45 pp (in Italian)

Duan Z, Sun R (2003) An improved model calculating CO_2 solubility in pure water and aqueous NaCl solutions from 273 to 533 K and from 0 to 2000 bar. Chem Geol 193:257–271

Duchi V, Minissale A, Paolieri M, Prati F, Valori A (1992) Chemical relationship between discharging fluids in the Siena-Radicofani graben and the deep fluids produced by the geothermal fields of Mt. Amiata, Torre Alfina and Latera, central Italy. Geothermics 21:401–413

Edwards RL, Chen JH, Wasserburg GJ (1987) ^{238}U-^{234}U-^{230}Th-^{232}Th systematics and the precise measurement of time over the past 500,000 years. Earth Planet Sci Lett 81:175–192

El Desouky H, Soete J, Claes H, Özkul M, Vanhaecke F, Swennen R (2015) Novel applications of fluid inclusions and isotope geochemistry in unravelling the genesis of fossil travertine systems. Sedimentology 62:27–57

Faccenna C, Soligo M, Billi A, De Filippis L, Funiciello R, Rossetti C, Tuccimei P (2008) Late Pleistocene depositional cycles of the Lapis Tiburtinus travertine (Tivoli, Central Italy): possible influence of climate and fault activity. Global Planet Change 63:293–308

Fancelli R, Nuti S (1975) Studio sulle acque termali e minerali della parte orientale della provincia di Siena. Boll. Soc It 94:135–155

Ferrari L, Conticelli S, Burlamacchi L, Manetti P (1996) Volcanological evolution of the Monte Amiata, southern Tuscany: new geological and petrochemical data. Acta Vulcanol 8:41–56

Flügel E (2004) Microfacies of carbonate rocks. Analysis, interpretation and application. Springer, New York

Ford TD, Pedley HM (1996) A review of tufa and travertine deposits of the world. Earth Sci Rev 41:117–175

Fornaca Rinaldi G (1968) $^{230}Th/^{234}Th$ dating of cave concretions. Earth Planet Sci Lett 5:120–122

Fouke BW, Farmer JD, Des Marais DJ, Pratt L, Sturchio NC, Burns PC, Discipulo MK (2000) Depositional facies and aqueous-solid geochemistry of travertine-depositing hot springs (Angel Terrace, Mammoth Hot Springs, Yellowstone National Park, U.S.A.). J Sedim Res 70:565–585

Fournier RO (1985) Carbonate transport and deposition in the epithermal environment. In: Berger BR, Bethke PM (eds) Geology and geochemistry of epithermal systems, reviews in economic geology, vol 2, pp 63–71

Friedman I (1970) Some investigations on the deposition of travertine from hot springs—I. The isotopic chemistry of a travertine-depositing spring. Geochim Cosmochim Acta 34:1303–1315

Friedman I, O'Neil JR (1977) Compilation of stable isotope fractionation factors of geochemical interest. In: Fleischer M (ed) Data of geochemistry, 6th edn. US Geological Survey Professional Paper 440-KK, KK1–KK12

Fritz P (1965) Composizione isotopica dell'ossigeno e del carbonio nei travertini della Toscana. Boll Geofis Teor Appl 7:25–30

Frondini F, Caliro S, Cardellini C, Chiodini G, Morgantini N, Parello F (2008) Carbon dioxide degassing from Tuscany and Northern Latium (Italy). Global Planet Change 61:89–102

Frondini F, Caliro S, Cardellini C, Chiodini G, Morgantini N (2009) Carbon dioxide degassing and thermal energy release in the Monte Amiata volcanic-geothermal area (Italy). Appl Geochem 24:860–875

Gandin A, Capezzuoli E (2014) Travertine: distinctive depositional fabrics of carbonates from thermal spring systems. Sedimentology 61:264–290

Gasparrini M, Ruggieri G, Brogi A (2013) Diagenesis versus hydrothermalism and fluid–rock interaction within the Tuscan Nappe of the Monte Amiata CO_2-rich geothermal area (Italy). Geofluids 13:159–179

Gianelli G (2008) A comparative analysis of the geothermal fields of Larderello and Mt. Amiata, Italy. In: Ueckermann HI (ed) Geothermal energy research trends. Nova Science, New York, pp 59–85

Gianelli G, Puxeddu M, Batini F, Bertini G, Dini I, Pandeli E, Nicolich R (1988) Geological model of a young volcanoplutonic system: the geothermal region of Monte Amiata (Tuscany, Italy). Geothermics 17:719–734

Gibert RO, Taberner C, Sáez A, Giralt S, Alonso RN, Edwards RL, Pueyo JJ (2009) Igneous origin of CO_2 in ancient and recent hot-spring waters and travertines from the northern Argentinean Andes. J Sediment Res 79:554–567

Goldstein RH, Reynolds TJ (1994) Fluid inclusion microthermometry. In: Systematics of fluid inclusions in diagenetic minerals. Society for Sedimentation Geology. Short course 31, pp 87–121

Gonfiantini R, Panichi C, Tongiorgi E (1968) Isotopic disequilibrium in travertine deposition. Earth Planet Sci Lett 5:55–58

Gudmundsson A, Fjeldskaar I, Brenner SL (2002) Propagation pathways and £uid transport of hydrofractures in jointed and layered rocks in geothermal fields. J Volcanol Geoth Res 116:257–278

Guo L, Riding R (1998) Hot-spring travertine facies and sequences, Late Pleistocene, Rapolano Terme, Italy. Sedimentology 45:163–180

Guo L, Riding R (1999) Rapid facies changes in Holocene fissure ridge hot spring travertines, Rapolano Terme, Italy. Sedimentology 46:1145–1158

Guo L, Andrews J, Riding R, Dennis P, Dresser Q (1996) Possible microbial effects on stable carbon isotope in hot spring travertine. J Sediment Res 66:468–473

Hancock PL, Chalmers RML, Altunel E, Çakir Z (1999) Travitonics: using travertines in active fault studies. J Struct Geol 21:903–916

Hedenquist JW, Henley RW (1985) Hydrothermal eruptions in the Waiotapu Geothermal System, New-Zealand—their origin, associated breccias, and relation to precious metal mineralization. Econ Geol 80:1640–1668

Hubbert MK, Willis DG (1957) Mechanics of hydraulic fracturing. Trans Inst Min Metall Pet Eng 210:165–166

Jones B, Renaut RW, Rosen MR (1996) High-temperature (>90°C) calcite precipitation at Waikite Hot Springs, North Island, New Zealand. J Geol Soc London 153:481–496

Kele S, Demény A, Siklósy Z, Németh T, Mária T, Kóvacs MB (2008) Chemical and stable isotope compositions of recent hot-water travertines and associated thermal waters, from Egerszalók, Hungary: depositional facies and non-equilibrium fractionations. Sed Geol 211:53–72

Kele S, Özkul M, Gökgöz A, Fórizs I, Baykara MO, Alçiçek MC, Németh T (2011) Stable isotope geochemical and facies study of Pamukkale travertines: new evidences of low-temperature non-equilibrium calcite-water fractionation. Sed Geol 238:191–212

Kerrich R (1986) Fluid infiltration into fault zones: chemical, isotopic, and mechanical effects. Pure Appl Geochem 124:225–268

Laurenzi MA, Villa IM (1991) The age or the early volcanic activity at Monte Amiata volcano, Tuscany: evidence for a paleomagnetic reversal at 300 Ka bp. Plinius 6:160–161

Liotta D, Ruggieri G, Brogi A, Fulignati P, Dini A, Nardini I (2009) Migration of geothermal fluids in extensional terrains: the ore deposits of the Boccheggiano-Montieri area (Southern Tuscany, Italy). Int J Earth Sci (Geol Rundsch) 99:623–644

Longinelli A, Selmo E (2003) Isotopic composition of precipitation in Italy: a first overall map. J Hydrol 270:75–88

Ludwig KR (1999) User's Manual for Isoplot/Ex Version 2.02, a geochronological toolkit for Microsoft Excel. Berkeley Geochronology Center Special Publication 1a. Berkeley, CA, USA

Malesani P, Vannucci S (1975) Precipitazione di calcite o di aragonite dalle acque termo-minerali in relazione alla genesi e alla evoluzione dei travertini. Rend Acc Naz Lincei 58:761–776

Manfra L, Masi U, Turi B (1974) Effetti isotopici nella diagenesi dei travertini. Geol Rom 13:147–155

Manfra L, Masi U, Turi B (1976) La composizione isotopica dei travertini del Lazio. Geol Rom 15:127–174

Marinelli G (1969) Some geological data on the geothermal area of Tuscany. Bull Vulcanol 33(1):319–334

McCrea JM (1950) On the isotope chemistry of carbonates and a palaeotemperature scale. J Chem Phys 18:849–857

Minissale A (2004) Origin, transport and discharge of CO_2 in central Italy. Earth Sci Rev 66:89–141

Minissale A, Evans WC, Magro G, Vaselli O (1997) Multiple source components in gas manifestations from north-central Italy. Chem Geol 142:175–192

Minissale A, Vaselli O, Tassi F, Magro G, Grechi GP (2002) Fluid mixing in carbonate aquifers near Rapolano (central Italy): chemical and isotopic constraints. Appl Geochem 17:1329–1342

Molli G (2008) Northern Apennine-Corsica orogenic system: an updated overview. Geol Soc Lond Spec Publ 298:413–442

Panichi C, Tongiorgi E (1976) Carbon isotopic composition of CO_2 from springs, fumaroles, mofettes, and travertines of Central and Southern Italy: a preliminary prospection method of geothermal area. In: Proceedings 2nd UN symposium on the development and use of geothermal resources, 20–29 May 1975, San Francisco, pp 815–825

Peccerillo A (2003) Plio-Quaternary magmatism in Italy. Episodes 26:222–226

Pentecost A (2005) Travertine. Springer, Heidelberg, pp 101–147

Renaut RW, Jones B (1997) Controls on aragonite and calcite precipitation in hot spring travertine at Chemurkeu, Lake Bogoria, Kenya. Can J Earth Sci 34:801–816

Renaut RW, Owen RB, Jones B, Tiercelin J-J, Tarits C, Ego JK, Konhauser KO (2013) Impact of lake-level changes on the formation of thermogene travertine in continental rifts: evidence from Lake Bogoria, Kenya Rift Valley. Sedimentology 60:428–468

Richardson CK, Holland HD (1979) Fluorite deposition in hydrothermal systems. Geochem Cosmochim Acta 43:1327–1335

Riding R (1991) Classification of microbial carbonates. In: Riding R (ed) Calcareous algae and stromatolites. Springer, Berlin, pp 21–51

Rimondi V, Chiarantini L, Lattanzi P, Benvenuti M, Beutel M, Colica A, Costagliola P, Di Benedetto F et al (2015) Metallogeny, exploitation and environmental impact of the Mt. Amiata mercury ore district (Southern Tuscany, Italy). It J Geosci (in press)

Roedder E (1970) Application of an improved crushing microscope stage to the studies of the gases in fluid inclusions. Schweiz Mineral Petrogr Mitt 50:41–58

Roedder E (1984) Fluid inclusions. In: Ribbe PH (ed) Reviews in mineralogy, vol 12. Mineralogical Society of America, Washington, DC

Rogie J, Kerrick DM, Chiodini G, Frondini F (2000) Flux measurements of nonvolcanic CO_2 emission from some vents in central Italy. J Geophys Res 105:8435–8445

Ruggieri G, Gianelli G (1999) Multi-stage fluid circulation in a hydraulic fracture breccia of the Larderello geothermal field Italy. J Volcanol Geoth Res 90:241–261

Sasada M (1985) CO_2-bearing fluid inclusions from geothermal field. Geotherm Resour Counc Trans 9:351–356

Shepherd TJ, Rankin AH, Alderton DHM (1985) A practical guide to fluid inclusion studies. Blackie, Glasgow

Simmons SF, Christenson WB (1994) Origins of calcite in a boiling geothermal system. Am J Sci 294:361–400

Słowakiewicz M (2003) Fluid inclusion data from the Upper Triassic hot-spring travertines in southern Poland. J Geochem Explor 78–79:123–126

Taddeucci A, Voltaggio M (1987) Th-230 dating of the travertines connected to the Vulsini Mts. volcanism (Northern Latium, Italy): neotectonics and hydrogeology. Per Mineral 56:295–302

Tanelli G (1983) Ore deposits and minerogenesis of Tuscany. Mem Soc Geol Ital 25:91–106 **(in Italian)**

Tassi F, Vaselli O, Cuccoli F, Buccianti A, Nisi B, Lognoli E, Montegrossi G (2009) A geochemical multi-methodological approach in hazard assessment of CO_2-rich gas emissions at Mt. Amiata Volcano (Tuscany, Central Italy). Water Air Soil Pollut Focus 9:117–127

Turi B (1986) Stable isotopes geochemistry of travertines. In: Fritz P, Fontes JC (eds) The terrestrial environment. Handbook of environmental isotope geochemistry, vol 2B. Elsevier, Amsterdam, pp 207–238

Uysal IT, FengY Zhao J-X, Altunel E, Weatherley D, Karakacak V, Cengiz O, Golding SD, Lawrence MG, Collerson KD (2007) U-series dating and geochemical tracing of late Quaternary travertine in co-seismic fissures. Earth Planet Sci Lett 257:450–462

Uysal IT, Feng Y-X, Zhao J-X, Isik V, Nuriel P, Golding SD (2009) Hydrothermal CO_2 degassing in seismically active zones during the late Quaternary. Chem Geol 265:442–454

Vermoere M, Degryse P, Vanhecke L, Muchez Ph, Paulissen E, Smets E, Waelkens M (1999) Pollen analysis of two travertine sections in Basköy (southwestern Turkey): implications for environmental conditions during the early Holocene. Rev Palaeobot Palyno 105:93–110

Winkel LHE, Casentini B, Bardelli F, Voegelin A, Nikolaidis NP, Charlet L (2013) Speciation of arsenic in Greek travertines: coprecipitation of arsenate with calcite. Geochimic Cosmochim Acta 106:99–110

Zhao J-X, Hu K, Collerson KD, Xu HK (2001) Thermal ionization mass spectrometry U-series dating of a hominid site near Nanjing, China. Geology 29:27–30

Zheng Y-Z (1990) Carbon-oxygen isotopic covariation in hydrothermal calcite during degassing of CO_2. A quantitative evaluation and application to the Kushikino gold mining area in Japan. Mineral Depos 25:246–250

Zhou HY, Zhao J-X, Wang Q, Feng Y-X, Tang J (2011) Speleothem-derived Asian summer monsoon variations in Central China during 54–46 ka. J Quat Sci 26:781–790